Journal of Mathematical Biology (2025) 91:55
https://doi.org/10.1007/s00285-025-02278-x

Mathematical Biology

Effects and biological consequences of the predator-mediated apparent competition II: PDE models

Yuan Lou[1] · Weirun Tao[2] · Zhi-An Wang[3]

Received: 8 February 2025 / Revised: 20 July 2025 / Accepted: 29 August 2025 /
Published online: 13 October 2025

Abstract

In Lou et al. (Lou Y, Tao W, Wang Z-A. Effects and biological consequences of the predator-mediated apparent competition I: ODE models. J. Math. Biol. 91 (2025), 47, 37 pages), the authors investigated the effects and biological consequences of the predator-mediated apparent competition using a temporal (ODE) system consisting of one predator and two prey species (one is native and the other is invasive) with Holling type I and II functional responses. This paper is a sequel to Lou et al. (Lou Y, Tao W, Wang Z-A. Effects and biological consequences of the predator-mediated apparent competition I: ODE models. J. Math. Biol. 91 (2025), 47, 37 pages.), by including spatial movements (diffusion and prey-taxis) into the ODE system and examining the spatial effects on the population dynamics under the predator-mediated apparent competition. We establish the global boundedness of solutions in a two-dimensional bounded domain with Neumann boundary conditions and the global stability of constant steady states in certain parameter regimes, by which we find a threshold dynamics in terms of the predator's death rate. For the parameters outside the global stability regimes, we conduct a linear stability analysis to show that diffusion and/or prey-taxis can induce instability by both steady-state and Hopf bifurcations. We further use numerical simulations to illustrate that various spatial patterns are all possible, including stable spatial aggregation patterns, spatially homogeneous but time-periodic patterns, and spatially inhomogeneous and time-oscillatory patterns. It comes with a surprise that either of diffusion and prey-taxis can induce steady-state or Hopf bifurcations to generate intricate spatial patterns in the one predator-two prey system, which

✉ Zhi-An Wang
mawza@polyu.edu.hk

Yuan Lou
yuanlou@sjtu.edu.cn

Weirun Tao
taoweiruncn@163.com

1 School of Mathematical Sciences, Shanghai Jiao Tong University, Shanghai 200240, China

2 School of Mathematics, Southeast University, Nanjing 211189, China

3 Department of Applied Mathematics, The Hong Kong Polytechnic University, Hung Hom, Hong Kong

is sharply different from the one predator-one prey system for which neither diffusion nor prey-taxis can induce spatial patterns. These results show that spatial movements play profound roles in the emerging properties for predator-prey systems with multiple prey species. We also find that prey-taxis may play dual roles (stabilization and destabilization) and facilitate the predator-mediated apparent competition to eliminate the native prey species under the moderate initial mass of invasive prey species.

Keywords Predator-mediated · Apparent competition · Prey-taxis · Global stability

Mathematics Subject Classification Primary 35B40 · 35K57 · 35Q92 · 92D25

1 Introduction

Predation and competition have long been a major study of interest in the field of ecology, partially because they form the foundational elements upon which complex, multispecies food webs are constructed (cf. DeAngelis 2012; Polis and Winemiller 2013; Holt and Polis 1997). Predation plays an important role in maintaining biodiversity and shaping the stable structure of ecology. For instance, in the absence of effective predator regulation, prey populations may over-reproduce and exceed the carrying capacity, leading to the depletion of smaller animal populations, the degradation of plant communities, and damage to fragile ecosystems like coral reefs (see https://blog.biodiversitylibrary.org/2012/08/why-predators-protect-biodiversity.html). Competition can happen between different species (interspecific competition) or among the same species (intraspecific competition) directly or indirectly. Among them is the predator-mediated apparent competition (cf. Holt 1977; Holt and Bonsall 2017): negative indirect interactions between prey species that are mediated by the shared natural predator. In one predator-one prey systems, predators can not drive the prey species to extinction since they would starve to death before they can find the last prey species. However, if they are fed by another prey (viewed as an invasive prey species), they may keep native prey species at a lower abundance level or even eliminate the native prey species through the predator-mediated apparent competition. For instance, populations of the damaging Pacific mites (pest) were reduced when both herbivorous Willamette mites and predatory mites were released together, which can not be achieved by releasing predatory mites alone (cf. Karban et al. 1994). Besides the above examples, apparent competition can be used in biological control (Chailleux et al. 2014; Kaser and Ode 2016; George 2017), conservation (Wittmer et al. 2013), and infectious disease ecology and invasion (Dunn et al. 2012; Strauss et al. 2012). For more applications of the predator-mediated apparent competition, we refer readers to (Chaneton and Bonsall 2000; Stige et al. 2018; Karban et al. 1994; DeCesare et al. 2010) and references therein.

Although many interspecific competitions are detectable (cf. Tilman 1987), apparent competition is difficult to detect or measure due to its indirect nature (Stige et al., 2018). Therefore, it is imperative to construct appropriate mathematical models to understand or predict the underlying qualitative or quantitative dynamics. The prototypical predator-mediated apparent competition model with i-species ($i \in \mathbb{N}_+$) was

introduced by Holt in Holt (1977) and later discussed in Holt and Bonsall (2017) as follows

$$\begin{cases} \frac{du_i}{dt} = u_i \left[g_i(u_i) - f_i(\mathbf{u}) w \right], \\ \frac{dw}{dt} = w F(\mathbf{u}), \end{cases} \tag{1.1}$$

where w and u_i represent the densities of the predator and the i-th prey species respectively, and $\mathbf{u} = (u_1, u_2, \ldots, u_i)$. In the first equation of (1.1), the function $g_i(u_i)$ denotes the inherent per capita growth rate of the i-th prey species in the absence of the predator, $f_i(\mathbf{u})$ is the functional response of the predator to the i-th prey species while $f_i(\mathbf{u})w$ representing per capita death rate caused by predation. In the second equation of (1.1), $F(\mathbf{u})$ denotes the per capita growth rate of the predator. Under the assumption that there is no direct interspecific competition between prey species, it was found in Holt (1977) that an increase in the abundance of one prey species benefits the predator, which in turn negatively affects prey species, resulting in lower abundances for each prey. The related one predator-two prey ordinary differential systems have been studied in the literature (cf. Vance 1978; Piltz et al. 2017; Mimura and Kan-on 1986; Hsu 1981; Caswell 1978; Abrams 1999) to qualitatively explore the predator-mediated coexistence or extinction. Among others, the research of this paper is related to the following one predator-two prey model describing the predator-mediated apparent competition

$$\begin{cases} u_t = u\,(1 - u/K_1) - w f_1(u), & t > 0, \\ v_t = v\,(1 - v/K_2) - w f_2(v), & t > 0, \\ w_t = w\,(\beta_1 f_1(u) + \beta_2 f_2(v) - \theta)\,, & t > 0, \end{cases} \tag{1.2}$$

where $u(t)$, $v(t)$ and $w(t)$ represent the densities of the native prey species, the invasive prey species, and the shared predator species at time t, respectively. The functions f_i $(i = 1, 2)$ and the positive parameters in (1.2) have the following biological interpretations:

- f_i $(i = 1, 2)$ - functional responses;
- K_i $(i = 1, 2)$ - carrying capacities for the prey;
- β_i $(i = 1, 2)$ - trophic efficiency (conversion rates);
- θ - death rate of the predator.

Based on (1.2), it is shown by the authors in Lou et al. (2025) that the predator-mediated apparent competition can indeed reduce the biomass of the native prey species. Moreover, whether the invasive prey species successfully invades or not essentially depends on its initial biomass while functional responses and other factors like the death rate of the predator may also play roles.

The effect of spatial dispersal of biological species was not considered in Lou et al. (2025). It is well-known that dispersal, an ecological process involving the spatial movement of individual/multiple species, is a strategy to increase species fitness in a heterogeneous landscape by regulating the dynamics and persistence of populations, the distribution and abundance of species as well as community structure (Hiltunen

and Laakso 2013; Holt 1977; Dieckmann et al. 1999). The causes and consequences as well as the selection and evolution of dispersal strategies have been central questions in ecology extensively discussed in the literature (cf. Cosner 2014; Shurin and Allen 2001; Ron et al. 2018). Dispersal is an indispensable factor in accurately finding and predicting population dynamics in a realistic ecosystem. Usually, dispersal can be classified into two categories: undirected movement (i.e. diffusion) and directed movement (advection). Among many remarkable mathematical works, a prominent finding is that diffusion can increase population abundance in a single-species community (Lou 2006) and the slower diffuser will outcompete its faster competitor (De Mottoni 1979; Lou 2006; He and Ni 2016). The main goal of this paper is to include spatial dispersal into the ODE model (1.2) and investigate the effects of dispersal on the population dynamics in one predator-two prey systems with apparent competition mediated by predators. Since (1.2) describes the apparent competition between two prey species mediated by one predator, it is natural to consider the prey-taxis (the directed movement of a predator up a prey density gradient) apart from the random diffusion. Therefore we are motivated to consider the following PDE system:

$$\begin{cases} u_t = d_1\Delta u + u\,(1-u/K_1) - wf_1(u), & x\in\Omega,\ t>0,\\ v_t = d_2\Delta v + v\,(1-v/K_2) - wf_2(v), & x\in\Omega,\ t>0,\\ w_t = d_3\Delta w - \nabla\cdot(w\,(\chi_1\nabla u + \chi_2\nabla v))\\ \qquad +w\,(\beta_1 f_1(u) + \beta_2 f_2(v) - \theta)\,, & x\in\Omega,\ t>0,\\ \partial_\nu u = \partial_\nu v = \partial_\nu w = 0, & x\in\partial\Omega,\ t>0,\\ (u,v,w)(x,0) = (u_0,v_0,w_0)(x), & x\in\Omega, \end{cases} \tag{1.3}$$

where the habitat $\Omega\subset\mathbb{R}^n$ ($n\geq 2$) is a bounded domain with smooth boundary $\partial\Omega$, $\partial_\nu := \frac{\partial}{\partial\nu}$ and ν is the outward unit normal vector of $\partial\Omega$. The functions $u(x,t)$, $v(x,t)$ and $w(x,t)$ represent the densities of the native prey species, the invasive prey species, and the shared predator at location x and time t, respectively. The functions f_i and the parameters K_i, β_i ($i=1,2$) and θ have the same biological interpretations as given above. The parameters d_1, d_2, d_3 denote the diffusion rates of the native prey, the invasive prey, and the predator, respectively, and $\chi_i (i=1,2)$ measures the prey-taxis intensity. All the parameters in (1.3) are positive except for $\chi_1, \chi_2 \geq 0$. Here we assume that both prey species move randomly within the habitat Ω, while the predator undergoes random diffusion and prey-taxis. Homogeneous Neumann boundary conditions mean that no individuals can cross the boundary. In the model (1.3), the direct (i.e. interference) competition between two prey species is not considered since we focus on the predator-mediated apparent competition here. Without loss of generality, we assume that the functional responses f_1 and f_2 are of the Holling type:

$$f_i(s) = \alpha_i s, \qquad i=1,2,\ \text{(Holling type I)}, \tag{1.4}$$

$$\text{or}\quad f_i(s) = \frac{\gamma_i s}{1+\gamma_i h_i s},\quad i=1,2,\ \text{(Holling type II)}, \tag{1.5}$$

where the positive constants α_i, γ_i and h_i ($i=1,2$) have the following biological meanings:

- α_i, γ_i $(i = 1, 2)$ - capture rates of the predator on the prey;
- h_i $(i = 1, 2)$ - handling time spent by the predator on the prey.

The spatial predator-prey systems with diffusion involving one predator and two prey species have been considered (Chin-Chin 2019; Huang and Lin 2014; Manna et al. 2020; Feng 1993; Lakoš 1990). However, all these studies focused on direct competition between the two prey species and did not consider prey-taxis in particular. In Haskell and Bell (2020), the negative prey-taxis (the directed movement of a predator down a prey density gradient) to one prey was considered and the global existence of solutions along with pattern formation was established in one dimension. In Apreutesei et al. (2014), an optimal control problem related to the system (1.3) with $\chi_1 = \chi_2 = 0$ is investigated to maximize the total biomass of the three species. As far as we know, the system (1.3) with (positive) prey-taxis on two prey species has not been studied in the literature. The goal of this paper is twofold: to establish the global well-posedness (existence and stability) of solutions to (1.3), and to investigate the effects of spatial movements brought to the population distribution profiles and outcome of the predator-mediated apparent competition. By studying the ODE counterpart of (1.3) in our previous work Lou et al. (2025), we find that the effects and biological consequences of predator-mediated apparent competition are a complicated ecological process depending upon many factors such as the initial mass of invasive prey species, the mortality rate of the predator and the mechanism of functional responses. In addition to the global well-posedness of (1.3), we shall further explore the following two questions. The first one is

Q1: Will spatial movements (diffusion or prey-taxis) facilitate or impede the effectiveness of the predator-mediated apparent competition?

It is well-known that neither diffusion nor prey-taxis can induce spatial pattern formation in one predator-one prey systems with Holling I or II functional responses (see Appendix A). Hence our second question will be

Q2: Will spatial movements (diffusion or prey-taxis) induce the instability to generate the spatial patterns in the one predator-two prey system?

This paper will focus on questions **Q1** and **Q2** alongside the global well-posedness of (1.3). The rest of this paper is organized as follows. Sect. 2 states the mathematical results on the global existence, boundedness, and the large time behavior of solutions to the system (1.3), as well as the biological implications concerning questions **Q1** and **Q2** based on our analytical and numerical simulations. In Sect. 3, we present the proofs for our analytical results stated in Sect. 2. The linear stability analysis is conducted in Sect. 4 to determine the parameter regimes in terms of diffusion and prey-taxis coefficients in which the steady-state or Hopf bifurcation occurs. On top of this, the numerical simulations are performed in Sect. 5 to show that either diffusion or prey-taxis can generate intricate patterns, including stable non-constant steady states, spatially inhomogeneous or heterogeneous but time-periodic patterns. In Sect. 6, we conclude our paper with a summary and discussion.

2 Main results and biological implications

Our main results consist of two parts: analytical results and biological implications based on linear stability analysis and numerical simulations. They shall be readily presented below.

2.1 Analytical results

For clarity and conciseness, we first introduce some notations used throughout the paper. Without confusion, we shall use $\int_\Omega f$ to denote $\int_\Omega f dx$. Moreover, we let

$$L_i := \beta_i f_i(K_i),\ \lambda_i := \tfrac{1}{\gamma_i h_i},\quad i = 1, 2,$$
$$L := L_1 + L_2,\quad \theta_0 := \max\left\{(1 - \tfrac{\alpha_1}{\alpha_2})L_1, (1 - \tfrac{\alpha_2}{\alpha_1})L_2\right\}.$$

We denote the constant steady state of the system (1.3) by $E_s = (u_s, v_s, w_s)$ including extinction, predator-free, semi-coexistence and coexistence steady states, as listed in Table 1 (cf. Lou et al. 2025). To distinguish the constant coexistence steady state for different functional responses, we employ the notation

$$E_* = \begin{cases} P_*, & \text{if (1.4) holds,} \\ Q_*, & \text{if (1.5.) holds.} \end{cases}$$

Moreover, for the Holling type I functional response (1.4), P_* is uniquely determined by

$$\begin{aligned} P_* &= (u_*, v_*, w_*) \\ &= \left(\frac{K_1\left[(\alpha_2 - \alpha_1)L_2 + \alpha_1\theta\right]}{\alpha_1 L_1 + \alpha_2 L_2}, \frac{K_2\left[(\alpha_1 - \alpha_2)L_1 + \alpha_2\theta\right]}{\alpha_1 L_1 + \alpha_2 L_2}, \frac{L - \theta}{\alpha_1 L_1 + \alpha_2 L_2}\right), \end{aligned}$$

which exists if and only if $\theta \in (\theta_0, L)$. However, the situation is more complicated for the Holling type II functional response (1.5), where the number of Q_* can vary from 0 to 3 (see Lou et al. 2025).

The first result concerns the global existence and boundedness of classical solutions to (1.3), as stated in the following theorem.

Theorem 2.1 *Let $\Omega \subset \mathbb{R}^N$ ($N \in \{1, 2\}$) be a bounded domain with smooth boundary, and let $(u_0, v_0, w_0) \in \left[W^{1,p}(\Omega)\right]^3$ with $u_0, v_0, w_0 \geq 0$ ($\not\equiv 0$) and $p > 2$. Then the system (1.3) with (1.4) or (1.5) has a unique global classical solution (u, v, w) satisfying $u, v, w > 0$ for all $t > 0$, and*

$$\|u(\cdot, t)\|_{L^\infty(\Omega)} + \|v(\cdot, t)\|_{L^\infty(\Omega)} + \|w(\cdot, t)\|_{L^\infty(\Omega)} \leq C \quad \text{for all } t > 0, \tag{2.1}$$

where $C > 0$ is a constant independent of t.

Remark 2.1 In Theorem 2.1, the growth functions for two prey are of logistic types $g_i(s) = s(1 - s/K_i)$ $(i = 1, 2)$, the functional response f_i $(i = 1, 2)$ are of Holling type I/II, and the predator mortality rate function only includes the natural death rate. The result can indeed be extended for more general functional responses (e.g. see (Jin and Wang 2017, Theorem 1.1) with general hypotheses).

We next give the global stability of the positive constant steady state $E_* = (u_*, v_*, w_*)$ for $0 < \theta < L$, and the predator-free constant steady state E_{uv} for $\theta \geq L$. If E_* exists, we define the positive constant

$$d_* := \begin{cases} \dfrac{w_*}{4}\left(\dfrac{\alpha_1\chi_1^2K_1^2}{\beta_1 d_1 f_1(u_*)} + \dfrac{\alpha_2\chi_2^2K_2^2}{\beta_2 d_2 f_2(v_*)}\right), & \text{if (1.4) holds,} \\ \dfrac{w_*}{4}\left(\dfrac{\gamma_1\chi_1^2K_1^2}{\beta_1 d_1 f_1(u_*)} + \dfrac{\gamma_2\chi_2^2K_2^2}{\beta_2 d_2 f_2(v_*)}\right), & \text{if (1.5) holds.} \end{cases} \tag{2.2}$$

The global stability results are stated below.

Theorem 2.2 (Global stability for Holling type I) *Let the assumptions in Theorem 2.1 hold with $f_i (i = 1, 2)$ given by (1.4). Let (u, v, w) be the solution of (1.3) obtained in Theorem 2.1 and d_* be given by (2.2). Then the following global stability results hold.*

(i) If $\theta \in (\theta_0, L)$, then the unique positive constant steady state P_* is globally asymptotically stable if $d_3 \geq d_*$, where "=" holds only if $\|u_0\|_{L^\infty(\Omega)} \leq K_1$ and $\|v_0\|_{L^\infty(\Omega)} \leq K_2$.

(ii) If $\theta \geq L$, then the predator-free constant steady state E_{uv} is globally asymptotically stable.

Theorem 2.3 (Global stability for Holling type II) *Assume the assumptions in Theorem 2.1 hold with $f_i (i = 1, 2)$ given by (1.5). Let (u, v, w) be the solution of (1.3) obtained in Theorem 2.1 and d_* be given by (2.2). Then the following global stability results hold.*

(i) If $\theta \in (0, L)$, and $Q_* = (u_*, v_*, w_*)$ is a positive constant steady state (if exists) satisfying

$$(K_1, K_2) \in \Lambda_* := \left\{(K_1, K_2) \;\middle|\; K_1 \leq \lambda_1 + u_*,\ K_2 \leq \lambda_2 + v_*\right\}, \tag{2.3}$$

then Q_* is globally asymptotically stable if $d_3 \geq d_*$, where "=" holds only if $\|u_0\|_{L^\infty(\Omega)} \leq K_1$ and $\|v_0\|_{L^\infty(\Omega)} \leq K_2$.

(ii) If $\theta \geq L$, then the predator-free constant steady state E_{uv} is globally asymptotically stable.

2.2 Biological implications based on numerical simulations

Now we shall address questions raised in Q1 and Q2 by using linear stability analysis and numerical simulations.

Table 1 Constant steady states of the system (1.3) with (1.4) or (1.5)

Type		Expression	Necessary and sufficient condition
Extinction		$E_0 = (0, 0, 0)$	$\theta > 0$
Predator-free		$E_u = (K_1, 0, 0),\ E_v = (0, K_2, 0),\ E_{uv} = (K_1, K_2, 0)$	$\theta > 0$
Semi-coexistence	(1.4)	$P_1 = (u_{P_1}, 0, w_{P_1}) = \left(\frac{\theta}{\alpha_1\beta_1}, 0, \frac{L_1-\theta}{\alpha_1 L_1}\right)$	$0 < \theta < L_1$
		$P_2 = (0, v_{P_2}, w_{P_2}) = \left(0, \frac{\theta}{\alpha_2\beta_2}, \frac{L_2-\theta}{\alpha_2 L_2}\right)$	$0 < \theta < L_2$
	(1.5)	$Q_1 = (u_{Q_1}, 0, w_{Q_1}) = \left(\frac{\theta}{(\beta_1-h_1\theta)\gamma_1}, 0, \frac{\beta_1(L_1-\theta)}{\gamma_1 f_1(K_1)(\beta_1-h_1\theta)^2}\right)$	$0 < \theta < L_1$
		$Q_2 = (0, v_{Q_2}, w_{Q_2}) = \left(0, \frac{\theta}{(\beta_2-h_2\theta)\gamma_2}, \frac{\beta_2(L_2-\theta)}{\gamma_2 f_2(K_2)(\beta_2-h_2\theta)^2}\right)$	$0 < \theta < L_2$
Coexistence	(1.4)	P_*	$\theta_0 < \theta < L$
	(1.5)	Q_*	Unclear*

Note: *For the existence of Q_*, it is hard to determine the necessary and sufficient conditions, and $0 < \theta < L$ is a necessary but not sufficient condition (see (Lou et al. 2025, Remark 2.1) for details)

By viewing one prey u and the predator w as the native species, and the other prey v as the invasive one in (1.3), we consider Holling type I and II functional responses and establish the global stability of the coexistence (i.e. positive) and the predator-free constant steady states in Theorem 2.2 and Theorem 2.3, respectively. By these results, we find threshold dynamics in terms of the predator's death/mortality rate. To investigate the spatial pattern formation, we conduct linear instability analysis outside the parameter regimes of global stability given in Theorem 2.2 and Theorem 2.3 (see Sect. 4) and perform numerical simulations (see Sect. 5) for the system (1.3) with (1.4) or (1.5) to pinpoint the possible biological consequences resulting from the predator-mediated apparent competition. Our main findings are summarized below.

(f.1) For the Holling type I functional response (1.4), diffusion or prey-taxis can not destabilize system (1.3) to generate spatial patterns and the long-time dynamics of (1.3) are mainly determined by the reaction terms, similar to its ODE counterpart.

(f.2) For the Holling type II functional response (1.5), the spatial movements can have profound effects on the population dynamics of system (1.3). For the case of symmetric apparent competition (namely, the two prey species have the same ecological characteristics), we find the initial biomass of invasive prey species is crucial to determine whether the invasion is successful: small invasion biomass leads to failed invasion, moderate invasion biomass leads to successful invasion and species coexistence, while large invasion biomass results in successful invasion which further wipes out the native prey species (see Fig. 1). By comparing the numerical results shown in Fig. 1-(b) and Fig. 2-(b), we find that strong prey-taxis for the native prey species can help the invasive species outcompete the native prey species (i.e. eliminate the native prey species) through the predator-mediated apparent competition given the success of invasion with moderate initial invasion biomass. This implies that prey-taxis can help the invasive prey species wipe out the native prey species with moderate invasion biomass only through the predator-mediated apparent competition.

(f.3) It is known that neither diffusion nor prey-taxis can destabilize one predator-one prey systems (see Appendix A) with Holling type I or II functional responses to promote the spatial pattern formations. However, for the one predator-two prey system (1.3) with the Holling type II functional response, we find that either diffusion or prey-taxis can destabilize positive uniform equilibria (see Table 6 and Fig. 4) to produce intricate spatial patterns (see Figs. 3 and 5). This finding entails that the effect of diffusion or prey-taxis may be substantially different as the number of prey species increases. Namely, spatial movements may play more profound roles in predator-prey systems with more prey species.

(f.4) In the one predator-two prey spatial system (1.3) with the Holling type II functional response, either diffusion or prey-taxis can destabilize positive equilibria to generate spatial patterns in some parameter regimes (see Remark 5.3). However, the prey-taxis may also stabilize (or homogenize) the system in other parameter regimes (see Figs. 4 and 5). Therefore the prey-taxis have different effects (stabilization and destabilization) depending on the suitable values of χ_1 and

χ_2 (i.e. the intensity of prey-taxis), indicating that spatial movements may play complex roles in predator-prey systems consisting of multiple prey species.

In this paper we attempt to understand the structures and functions of predator-prey systems with apparent competition and spatial movement. To summarize, our studies reveal some emerging properties of predator-mediated apparent competition models with movement: First, for symmetric apparent competition there exist critical thresholds for the initial biomass of the invasive prey species to determine whether the invasion is successful, and whether it will wipe out the native prey species. Second, spatial movement can induce spatiotemporal patterns in one predator-two prey system, but not for one predator-one prey system. It will be of interest to further investigate the functions of these spatiotemporal patterns, making the connections between the structures of these ecological systems and the functions of such structures.

3 Global boundedness and stability

3.1 Global boundedness

We first prove Theorem 2.1 concerning the global existence and boundedness of solutions to the system (1.3) with either (1.4) or (1.5). The local existence of solutions can be established by using Amann's theorem (cf. Amann 1990, 1993). Additionally, the approach developed for one predator-one prey systems with prey-taxis in Jin and Wang (2017) can be adapted here to prove Theorem 2.1 with slight adjustments.

Lemma 3.1 *Let the assumptions in Theorem 2.1 hold. Then there exists some* $T_{max} \in (0, \infty]$ *such that the system (1.3) with (1.4) or (1.5) admits a unique classical solution*

$$(u, v, w) \in \left[C^0\left(\bar{\Omega} \times [0, T_{max})\right) \cap C^{2,1}\left(\bar{\Omega} \times (0, T_{max})\right)\right]^3$$

satisfying $u, v, w > 0$ *for all* $t > 0$. *Moreover, we have*

$$\text{either} \quad T_{max} = \infty, \quad \text{or} \quad \limsup_{t \nearrow T_{max}} \|w(\cdot, t)\|_{L^\infty(\Omega)} = \infty. \tag{3.1}$$

Lemma 3.2 *Let the assumptions in Theorem 2.1 hold. Then for all* $t \in (0, T_{max})$, *the solution of the system (1.3) with (1.4) or (1.5) satisfies*

$$u \le M_1 := \max\left\{\|u_0\|_{L^\infty(\Omega)}, K_1\right\}, \quad v \le M_2 := \max\left\{\|v_0\|_{L^\infty(\Omega)}, K_2\right\}, \tag{3.2}$$

and

$$\|w\|_{L^1(\Omega)} \le M_3 := \max\left\{\beta_1\|u_0\|_{L^1(\Omega)} + \beta_2\|v_0\|_{L^1(\Omega)} + \|w_0\|_{L^1(\Omega)}, \frac{(1+\theta)^2}{4\theta}\left(\beta_1 K_1 + \beta_2 K_2\right)|\Omega|\right\}.$$

Proof Note that (3.2) is a direct consequence of (Jin and Wang 2017, Lemma 2.2) based on a comparison principle. We next prove the boundedness of $\|w\|_{L^1(\Omega)}$. Let

$$z(x,t) := \beta_1 u(x,t) + \beta_2 v(x,t) + w(x,t) \quad \text{for all } (x,t) \in \Omega \times (0, T_{max}).$$

Then using (1.3), integrating by parts, and Young's inequality, we have

$$\begin{aligned}\frac{d}{dt}\int_\Omega z &= \beta_1 \int_\Omega \left(u - \frac{u^2}{K_1}\right) + \beta_2 \int_\Omega \left(v - \frac{v^2}{K_2}\right) - \theta \int_\Omega w \\ &\le \beta_1 \int_\Omega \left[-\theta u + \frac{K_1(1+\theta)^2}{4}\right] + \beta_2 \int_\Omega \left[-\theta v + \frac{K_2(1+\theta)^2}{4}\right] - \theta \int_\Omega w \\ &\le -\theta \int_\Omega z + \frac{(1+\theta)^2}{4}\left(\beta_1 K_1 + \beta_2 K_2\right)|\Omega| \quad \text{for all } t \in (0, T_{max}).\end{aligned}$$

An application of Grönwall's inequalitygives $\|z\|_{L^1(\Omega)} \le M_3$, which along with the non-negativity of the solution completes the proof. □

Lemma 3.3 *Let the assumptions in Theorem 2.1 hold. Then the solution to the system (1.3) with (1.4) or (1.5) satisfies*

$$\|u(\cdot,t)\|_{L^\infty(\Omega)} + \|v(\cdot,t)\|_{L^\infty(\Omega)} + \|w(\cdot,t)\|_{L^\infty(\Omega)} \le C \quad \textit{for all } t \in (0, T_{max}), \tag{3.3}$$

where C is a positive constant independent of t.

Proof Based on Lemma 3.2, (3.3) can be established by similar arguments as in (Jin and Wang 2017, section 3) for one predator-one prey systems with prey-taxis. Here the two prey species bring no essential difficulty in deriving (3.3) since there is no direct interaction between the two prey species. The routine procedures are omitted for brevity. □

Proof of Theorem 2.1 It follows immediately from (3.1) and (3.3) that $T_{max} = \infty$, which alongside (3.3) gives (2.1). The proof is completed. □

3.2 Global stability

This subsection is devoted to proving Theorem 2.2 and Theorem 2.3. Note that the constant steady states E_0, E_u and E_v are saddles, and E_{uv} is also a saddle for $\theta \in (0, L)$ (see Proposition 4.1). In this section, we shall construct appropriate Lyapunov functions to investigate the global stability of positive constant steady states for $0 < \theta < L$ and the predator-free constant steady state E_{uv} for $\theta \ge L$. We first give the following higher-order regularities of the solution to the system (1.3) with (1.4) or (1.5).

Lemma 3.4 *Let the assumptions in Theorem 2.1 hold, and let (u, v, w) be the solution of the system (1.3) with (1.4) or (1.5). Then for any given $\sigma \in (0, 1)$, there exists a positive constant C such that*

$$\begin{aligned}&\|u\|_{C^{2+\sigma,1+\frac{\sigma}{2}}(\bar{\Omega}\times[1,\infty))} + \|v\|_{C^{2+\sigma,1+\frac{\sigma}{2}}(\bar{\Omega}\times[1,\infty))}\\ &+\|w\|_{C^{2+\sigma,1+\frac{\sigma}{2}}(\bar{\Omega}\times[1,\infty))} \le C.\end{aligned}$$

Proof With (2.1), the conclusion can be proved by a bootstrap argument based on the L^p-estimate and the Schauder estimate (cf. Gary 1996). We omit the details for brevity. □

The following auxiliary lemma will be used to prove the global stability.

Lemma 3.5 (Wang 2018, Lemma 1.1) *Let $a \ge 0$ and $b > 0$ be two constants, $F(t) \ge 0$, $\int_a^\infty H(t)\mathrm{d}t < \infty$. Assume that $E \in C^1([a, \infty))$ is bounded from below and satisfies*

$$E'(t) \le -bF(t) + H(t) \quad \text{in } [a, \infty).$$

If $F \in C^1([a, \infty))$ and $F'(t) \le C$ in $[a, \infty)$ for some constant $C > 0$, or $F \in C^\theta([a, \infty))$ and $\|F\|_{C^\theta([a,\infty))} \le C$ for some constants $0 < \theta < 1$ and $C > 0$, then $\lim_{t\to\infty} F(t) = 0$.

For $t > 0$ and a constant steady state $E_s = (u_s, v_s, w_s)$, we let

$$\begin{aligned}\mathcal{E}(t; E_s) := \Gamma_1 \int_\Omega \left(u - u_s - u_s \ln \frac{u}{u_s}\right) + \Gamma_2 \int_\Omega \left(v - v_s - v_s \ln \frac{v}{v_s}\right)\\ + \int_\Omega \left(w - w_s - w_s \ln \frac{w}{w_s}\right),\end{aligned} \tag{3.4}$$

where the positive constants Γ_1 and Γ_2 are given by

$$\Gamma_i := \begin{cases} \frac{\beta_i f_i(u_s)}{\alpha_i u_s} = \beta_i, & \text{if (1.4) holds,}\\ \frac{\beta_i f_i(u_s)}{\gamma_i u_s} = \frac{\beta_i}{1+\gamma_i h_i u_s}, & \text{if (1.5) holds,}\end{cases} \quad i = 1, 2. \tag{3.5}$$

Then we can prove the global stability of E_{uv} and the positive constant steady states, as to be shown below.

3.3 Global stability for $\theta \ge L$

The predator-free constant steady state E_{uv} of the system (1.3) with (1.4) or (1.5) is globally asymptotically stable whenever $\theta \ge L$.

Lemma 3.6 [Global stability of E_{uv}] *Let the assumptions in Theorem 2.1 hold, and let $\theta \ge L$. Then for any $\sigma \in (0, 1)$, the solution (u, v, w) of the system (1.3) with (1.4) or (1.5) satisfies*

$$\lim_{t\to\infty}\left(\|u-K_1\|_{C^{2+\sigma}(\bar{\Omega})}+\|v-K_2\|_{C^{2+\sigma}(\bar{\Omega})}+\|w\|_{C^{2+\sigma}(\bar{\Omega})}\right)=0.$$

Proof Let $E_s = E_{uv} = (K_1, K_2, 0)$ in (3.4) and (3.5). Then using (1.3), (3.4), (3.5), and integrating by parts, for all $t > 0$, one has

$$\begin{aligned}\mathcal{E}'(t;E_{uv}) = &\underbrace{-\Gamma_1 d_1 K_1\int_\Omega\frac{|\nabla u|^2}{u^2}-\Gamma_2 d_2 K_2\int_\Omega\frac{|\nabla v|^2}{v^2}}_{\le 0}\\ &+\int_\Omega w\left(\beta_1 f_1(u)+\beta_2 f_2(v)-\theta\right)\\ &+\Gamma_1\int_\Omega\left(1-\frac{u}{K_1}-\frac{wf_1(u)}{u}\right)(u-K_1)\\ &+\Gamma_2\int_\Omega\left(1-\frac{v}{K_2}-\frac{wf_2(v)}{v}\right)(v-K_2)\,.\end{aligned}\tag{3.6}$$

The combination of (1.4), (1.5), (3.5) and $\theta \ge L = \beta_1 f_1(K_1) + \beta_2 f_2(K_2)$ indicates that

$$\begin{aligned}w\left(\beta_1 f_1(u)+\beta_2 f_2(v)-\theta\right) &\le \beta_1 w\left(f_1(u)-f_1(K_1)\right)+\beta_2 w\left(f_2(v)-f_2(K_2)\right)\\ &=\Gamma_1\frac{wf_1(u)}{u}(u-K_1)+\Gamma_2\frac{wf_2(v)}{v}(v-K_2)\\ &\qquad\text{for all } t>0,\end{aligned}\tag{3.7}$$

where we have used the fact that $\beta_i(f_i(s)-f_i(K_i)) = \Gamma_i\frac{f_i(s)}{s}(s-K_i)$ for $s > 0$, $i = 1, 2$, since

$$\beta_i(f_i(s)-f_i(K_i))=\begin{cases}\alpha_i\beta_i(s-K_i)=\Gamma_i\frac{f_i(s)}{s}(s-K_i), & \text{if (1.4) holds,}\\ \frac{\gamma_i\beta_i(s-K_i)}{(1+\gamma_i h_i K_i)(1+\gamma_i h_i s)}=\Gamma_i\frac{f_i(s)}{s}(s-K_i), & \text{if (1.5) holds.}\end{cases}\tag{3.8}$$

Substituting (3.7) into (3.6), we obtain

$$\mathcal{E}'(t;E_{uv})\le-\frac{\Gamma_1}{K_1}\int_\Omega(u-K_1)^2-\frac{\Gamma_2}{K_2}\int_\Omega(v-K_2)^2=:-\mathcal{F}_1(t)\quad\text{for all } t>0.\tag{3.9}$$

For any constant $s_* > 0$, the function $\phi_1(s) := s - s_* - s_* \ln\frac{s}{s_*}$ satisfies $\phi_1(s) \ge \phi_1(s_*) = 0$ for $s > 0$, and $\phi_1(s) = 0$ if and only if $s = s_*$. Therefore, it holds that

$$\mathcal{E}(t;E_{uv})\ge 0\quad\text{for all } t>0.$$

This alongside Lemma 3.4 and Lemma 3.5 gives $\lim_{t\to\infty} \mathcal{F}_1(t) = 0$, namely

$$\lim_{t\to\infty} (\|u - K_1\|_{L^2(\Omega)} + \|v - K_2\|_{L^2(\Omega)}) = 0.$$

Take $\tilde{\sigma} \in (0, 1)$ satisfying $0 < \sigma < \tilde{\sigma} < 1$. Then Lemma 3.4 implies that $u(\cdot, t)$ and $v(\cdot, t)$ are bounded in $C^{2+\tilde{\sigma}}(\bar{\Omega})$ for $t \geq 1$ (since the embedding $C^{2+\tilde{\sigma}}\left(\bar{\Omega}\right) \hookrightarrow C^{2+\sigma}\left(\bar{\Omega}\right)$ is compact thanks to the Ascoli-Arzelà theorem). Using the compact arguments and uniqueness of limits (cf. (Bei 2011, Proof of Theorem 6.1 and Remark 6.1) for instance) we have

$$\lim_{t\to\infty} \left(\|u - K_1\|_{C^{2+\sigma}(\bar{\Omega})} + \|v - K_2\|_{C^{2+\sigma}(\bar{\Omega})}\right) = 0 \tag{3.10}$$

holds for any $\sigma \in (0, 1)$. It remains to prove

$$\lim_{t\to\infty} \|w\|_{C^{2+\sigma}(\bar{\Omega})} = 0. \tag{3.11}$$

Define $\bar{g}(t) = \frac{1}{|\Omega|}\int_\Omega g(x, t)\, dx$. Then by the first equation of (1.3), we have

$$\bar{u}'(t) = \frac{d}{dt}\left(\frac{1}{|\Omega|}\int_\Omega u\right) = \frac{1}{|\Omega|}\int_\Omega u\left(1 - \frac{u}{K_1}\right) - \frac{1}{|\Omega|}\int_\Omega w f_1(u) =: I_1(t) + I_2(t). \tag{3.12}$$

Clearly, (3.10) implies $I_1(t) \to 0$ as $t \to \infty$.

Lemma 3.4 implies $\|\bar{u}'\|_{C^{\sigma/2}([1,\infty))} \leq C$, which means that there exists a constant $C_\sigma > 0$ such that $|\bar{u}'(t) - \bar{u}'(s)| < C_\sigma |t - s|^{\frac{\sigma}{2}}$ for all $s, t \geq 1$. We claim $\lim_{t\to\infty} \bar{u}'(t) = 0$. Otherwise, there exists $\varepsilon > 0$ and a sequence $t_k \to \infty$ ($t_k \geq 1$) such that $|\bar{u}'(t_k)| > 2\varepsilon$ for all $k \in \mathbb{N}_+$. Clearly, for any $t \geq 1$ satisfying $|t - t_k| < (\varepsilon/C_\sigma)^{\frac{2}{\sigma}} =: \delta$ (note that δ is independent of k), we have

$$\begin{aligned} &|\bar{u}'(t) - \bar{u}'(t_k)| < \varepsilon \quad \text{and} \\ &\left|\bar{u}'(t)\right| \geq \left|\bar{u}'\left(t_k\right)\right| - \left|\bar{u}'(t) - \bar{u}'\left(t_k\right)\right| > \varepsilon. \end{aligned}$$

This along with $\bar{u}'(\cdot) \in C^{\sigma/2}([1, \infty))$ indicates that $\bar{u}'(t)$ will not change the sign in $[t_k, t_k + \delta]$. Using (3.10), we obtain

$$\begin{aligned} \delta\varepsilon \leq \int_{t_k}^{t_k+\delta} |\bar{u}'(x)| dx &= \left|\int_1^{t_k} \bar{u}'(x) dx - \int_1^{t_k+\delta} \bar{u}'(x) dx\right| \\ &= |\bar{u}\left(t_k\right) - \bar{u}\left(t_k + \delta\right)| \to 0 \quad \text{as } k \to \infty, \end{aligned}$$

which is a contradiction. The claim $\lim_{t\to\infty} \bar{u}'(t) = 0$ is proved. Hence (3.12) indicates that $\lim_{t\to\infty} I_2(t) = 0$, which gives

$$\lim_{t\to\infty} \int_\Omega w f_1(u) = 0. \tag{3.13}$$

Moreover, the combination of (2.1), (3.10) and Lemma 3.4 implies that

$$\left| \int_\Omega w\,[f_1(u) - f_1(K_1)] \right| \le C\|u - K_1\|_{L^1(\Omega)} \to 0 \quad \text{as } t \to \infty. \tag{3.14}$$

Therefore, we have from (3.13) and (3.14) that

$$0 = \lim_{t\to\infty} \int_\Omega w f_1(u) - \lim_{t\to\infty} \int_\Omega w\,[f_1(u) - f_1(K_1)] = f_1(K_1) \lim_{t\to\infty} \int_\Omega w,$$

namely $\lim_{t\to\infty} \|w\|_{L^1(\Omega)} = 0$. This combined with Lemma 3.4 yields (3.11) and completes the proof. □

3.4 Global stability for $\theta < L$

For $\theta \in (0, L)$, we consider the global stability of the positive constant steady states. We start with the Holling type I functional response (1.4) and give the global stability of P_*.

Lemma 3.7 (Global stability of P_*) *Assume that the assumptions in Theorem 2.1 hold with $f_1(u)$ and $f_2(v)$ given by (1.4), and (u, v, w) is the solution of system (1.3). Let d_* be given by (2.2), $\theta \in (\theta_0, L)$, and $P_* = (u_*, v_*, w_*)$ be the unique positive constant steady state of system (1.3). Then for any $\sigma \in (0, 1)$, it holds that*

$$\lim_{t\to\infty} \left(\|u - u_*\|_{C^{2+\sigma}(\bar{\Omega})} + \|v - v_*\|_{C^{2+\sigma}(\bar{\Omega})} + \|w - w_*\|_{C^{2+\sigma}(\bar{\Omega})} \right) = 0$$

if $d_3 \ge d_*$, where "=" holds in the case of $\|u_0\|_{L^\infty(\Omega)} \le K_1$ and $\|v_0\|_{L^\infty(\Omega)} \le K_2$.

Proof Let $E_s = P_* = (u_*, v_*, w_*)$ in (3.4) and (3.5). Then (3.5) implies $\Gamma_i = \beta_i$, $i = 1, 2$. Using (1.3), (1.4), (3.4), (3.5), the fact that

$$\theta = \beta_1 f_1(u_*) + \beta_2 f_2(v_*) = \alpha_1\beta_1 u_* + \alpha_2\beta_2 v_*, \quad 1 = \frac{u_*}{K_1} + \alpha_1 w_* = \frac{v_*}{K_2} + \alpha_2 w_*,$$

and integrating by parts, we have

$$\mathcal{E}'(t; P_*) = \underbrace{-\beta_1 d_1 u_* \int_\Omega \frac{|\nabla u|^2}{u^2} - \beta_2 d_2 v_* \int_\Omega \frac{|\nabla v|^2}{v^2} - d_3 w_* \int_\Omega \frac{|\nabla w|^2}{w^2} + w_* \int_\Omega (\chi_1 \nabla u + \chi_2 \nabla v) \cdot \frac{\nabla w}{w}}_{=: -\int_\Omega \aleph_1 \Xi_1 \aleph_1^T}$$

$$
\begin{aligned}
&+\beta_1\int_\Omega\left(1-\frac{u}{K_1}-\alpha_1 w\right)(u-u_*)+\beta_2\int_\Omega\left(1-\frac{v}{K_2}-\alpha_2 w\right)(v-v_*)\\
&+\int_\Omega(\alpha_1\beta_1 u+\alpha_2\beta_2 v-\theta)(w-w_*)\\
&=-\int_\Omega \aleph_1\Xi_1\aleph_1^T+\beta_1\int_\Omega\left(1-\frac{u}{K_1}-\alpha_1 w_*\right)(u-u_*)+\beta_2\int_\Omega\left(1-\frac{v}{K_2}-\alpha_2 w_*\right)(v-v_*)\\
&=-\int_\Omega \aleph_1\Xi_1\aleph_1^T-\frac{\beta_1}{K_1}\int_\Omega(u-u_*)^2-\frac{\beta_2}{K_2}\int_\Omega(v-v_*)^2\quad\text{for all } t>0,
\end{aligned}
\tag{3.15}
$$

where $\aleph_1:=(\nabla u,\nabla v,\nabla w)$ and

$$
\Xi_1:=\begin{pmatrix}
\frac{\beta_1 d_1 u_*}{u^2} & 0 & -\frac{\chi_1 w_*}{2w}\\
0 & \frac{\beta_2 d_2 v_*}{v^2} & -\frac{\chi_2 w_*}{2w}\\
-\frac{\chi_1 w_*}{2w} & -\frac{\chi_2 w_*}{2w} & \frac{d_3 w_*}{w^2}
\end{pmatrix}.
$$

By Sylvester's criterion, the matrix Ξ_1 is non-negative definite if and only if the determinant of Ξ_1 satisfies

$$
|\Xi_1|=\frac{\beta_1\beta_2 d_1 d_2 u_* v_* w_*}{u^2v^2w^2}\left[d_3-\frac{w_*}{4}\left(\frac{\chi_1^2u^2}{\beta_1 d_1 u_*}+\frac{\chi_2^2v^2}{\beta_2 d_2 v_*}\right)\right]\geq 0. \tag{3.16}
$$

On one hand, if $\|u_0\|_{L^\infty(\Omega)}\leq K_1$ and $\|v_0\|_{L^\infty(\Omega)}\leq K_2$, then we have from (2.2), (3.2) and (3.16) that

$$
|\Xi_1|\geq\frac{\beta_1\beta_2 d_1 d_2 u_* v_* w_*}{u^2v^2w^2}(d_3-d_*)\geq 0\quad\text{for all } (x,t)\in\bar\Omega\times(0,\infty).
$$

On the other hand, if $\|u_0\|_{L^\infty(\Omega)}>K_1$ or $\|v_0\|_{L^\infty(\Omega)}>K_2$, then the comparison principle (e.g., see (Jin and Wang 2017, Lemma 2.2) for details) shows that

$$
\limsup_{t\to\infty}u(x,t)\leq K_1\quad\text{and}\quad\limsup_{t\to\infty}v(x,t)\leq K_2\quad\text{for all } x\in\overline{\Omega}.
$$

This along with (2.2), (3.2), (3.16) and $d_3>d_*$ indicates that there exists $T_1>0$ such that $|\Xi_1|\geq 0$ for all $(x,t)\in\bar\Omega\times[T_1,\infty)$. Therefore, Ξ_1 is non-negative definite, and hence (3.15) indicates that

$$
\mathcal{E}'(t;P_*)\leq-\frac{\beta_1}{K_1}\int_\Omega(u-u_*)^2-\frac{\beta_2}{K_2}\int_\Omega(v-v_*)^2\quad\text{for all } t\geq T_1.
$$

We are now in the same situation as (3.9), and the remaining proof is omitted here for brevity since it is similar to that of Lemma 3.6. □

We next consider the Holling type II functional response (1.5), and give the global stability of Q_*.

Lemma 3.8 (Global stability of Q_*) *Assume that the assumptions in Theorem 2.1 hold with $f_1(u)$ and $f_2(v)$ given by (1.5), and (u,v,w) is the solution of the system (1.3).*

Let d_* be given by (2.2), $\theta \in (0, L)$, and $Q_* = (u_*, v_*, w_*)$ be a positive constant steady state of the system (1.3). Then for any $\sigma \in (0, 1)$, the conclusion

$$\lim_{t\to\infty} \left(\|u - u_*\|_{C^{2+\sigma}(\bar{\Omega})} + \|v - v_*\|_{C^{2+\sigma}(\bar{\Omega})} + \|w - w_*\|_{C^{2+\sigma}(\bar{\Omega})} \right) = 0$$

holds if $d_3 \geq d_*$, where "=" holds in the case of $\|u_0\|_{L^\infty(\Omega)} \leq K_1$ and $\|v_0\|_{L^\infty(\Omega)} \leq K_2$.

Proof Let $E_s = Q_* = (u_*, v_*, w_*)$ in (3.4) and (3.5). Then (3.5) implies $\Gamma_1 = \frac{\beta_1}{1+\gamma_1 h_1 u_*}$ and $\Gamma_2 = \frac{\beta_2}{1+\gamma_2 h_2 v_*}$. Using (1.3), (1.5), (3.4), (3.5), the fact that $\theta = \beta_1 f_1(u_*) + \beta_2 f_2(v_*)$, and integration by parts, we obtain

$$\begin{aligned}
\mathcal{E}'(t; Q_*) = & \underbrace{-\Gamma_1 d_1 u_* \int_\Omega \frac{|\nabla u|^2}{u^2} - \Gamma_2 d_2 v_* \int_\Omega \frac{|\nabla v|^2}{v^2} - d_3 w_* \int_\Omega \frac{|\nabla w|^2}{w^2} + w_* \int_\Omega (\chi_1 \nabla u + \chi_2 \nabla v) \cdot \frac{\nabla w}{w}}_{=: -\int_\Omega \aleph_2 \Xi_2 \aleph_2^T} \\
& + \Gamma_1 \int_\Omega \left(1 - \frac{u}{K_1} - \frac{w f_1(u)}{u}\right)(u - u_*) + \Gamma_2 \int_\Omega \left(1 - \frac{v}{K_2} - \frac{w f_2(v)}{v}\right)(v - v_*) \\
& + \beta_1 \int_\Omega (f_1(u) - f_1(u_*))(w - w_*) + \beta_2 \int_\Omega (f_2(v) - f_2(v_*))(w - w_*). \qquad (3.17)
\end{aligned}$$

Similar to (3.8), it holds that

$$\begin{aligned}
\beta_1 (f_1(u) - f_1(u_*)) &= \Gamma_1 \frac{f_1(u)}{u}(u - u_*) \quad \text{and} \\
\beta_2 (f_2(v) - f_2(v_*)) &= \Gamma_2 \frac{f_2(v)}{v}(v - v_*). \qquad (3.18)
\end{aligned}$$

Substituting (3.18) into (3.17), and using (2.3) and the fact that $w_* = \frac{u_*}{f_1(u_*)}(1 - \frac{u_*}{K_1}) = \frac{v_*}{f_2(v_*)}(1 - \frac{v_*}{K_2})$, we obtain

$$\begin{aligned}
\mathcal{E}'(t; Q_*) = & -\int_\Omega \aleph_2 \Xi_2 \aleph_2^T + \Gamma_1 \int_\Omega \left(1 - \frac{u}{K_1} - \frac{w_* f_1(u)}{u}\right)(u - u_*) \\
& + \Gamma_2 \int_\Omega \left(1 - \frac{v}{K_2} - \frac{w_* f_2(v)}{v}\right)(v - v_*) \\
= & -\int_\Omega \aleph_2 \Xi_2 \aleph_2^T - \int_\Omega \frac{\Gamma_1 h_1 \gamma_1 (\lambda_1 + u_* - K_1 + u)}{K_1 (1 + h_1 \gamma_1 u)}(u - u_*)^2 \\
& - \int_\Omega \frac{\Gamma_2 h_2 \gamma_2 (\lambda_2 + v_* - K_2 + v)}{K_2 (1 + h_2 \gamma_2 v)}(v - v_*)^2 \\
\leq & -\int_\Omega \aleph_2 \Xi_2 \aleph_2^T - \frac{\Gamma_1 h_1}{K_1} f_1(u)(u - u_*)^2 - \frac{\Gamma_2 h_2}{K_2} f_2(v)(v - v_*)^2,
\end{aligned}$$

where $\aleph_2 := (\nabla u, \nabla v, \nabla w)$ and

$$\Xi_2 := \begin{pmatrix} \frac{\Gamma_1 d_1 u_*}{u^2} & 0 & -\frac{\chi_1 w_*}{2w} \\ 0 & \frac{\Gamma_2 d_2 v_*}{v^2} & -\frac{\chi_2 w_*}{2w} \\ -\frac{\chi_1 w_*}{2w} & -\frac{\chi_2 w_*}{2w} & \frac{d_3 w_*}{w^2} \end{pmatrix}.$$

Then

$$|\Xi_2| = \frac{\Gamma_1\Gamma_2 d_1 d_2 u_* v_* w_*}{u^2 v^2 w^2}\left[d_3 - \frac{w_*}{4}\left(\frac{\chi_1^2 u^2}{\Gamma_1 d_1 u_*} + \frac{\chi_2^2 v^2}{\Gamma_2 d_2 v_*}\right)\right]$$
$$= \frac{\Gamma_1\Gamma_2 d_1 d_2 u_* v_* w_*}{u^2 v^2 w^2}\left[d_3 - \frac{w_*}{4}\left(\frac{\chi_1^2 u^2(1+\gamma_1 h_1 u_*)}{\beta_1 d_1 u_*} + \frac{\chi_2^2 v^2(1+\gamma_2 h_2 v_*)}{\beta_2 d_2 v_*}\right)\right].$$

The remaining proof can be completed by the arguments similar to those in the proof of Lemma 3.7, which we omit here for brevity. □

Proofs of Theorem 2.2 and Theorem 2.3 The combination of Lemma 3.6 and Lemma 3.7 proves Theorem 2.2. Moreover, Theorem 2.3 is a consequence of Lemma 3.6 and Lemma 3.8. □

4 Linear instability analysis

This section is dedicated to investigating possible Turing instability of the system (1.3) with (1.4) or (1.5) induced by spatial dispersal including diffusion and prey-taxis to explore the biological implications underlying the spatial patterns. Turing instability arises from a constant steady state that remains stable for the non-spatial system but destabilizes under spatial perturbations. For the one predator-one prey spatial system with the Holling type I (i.e. Lotka-Volterra) functional response and no flux boundary conditions, it is well-known that there is no spatially inhomogeneous pattern (De Mottoni and Rothe 1979; Du and Shi 2006), which remains unchanged in the presence of prey-taxis (Jin and Wang 2017, 2021). Moreover, there is no Turing instability either if the functional response is of Holling type II, see Appendix A for detailed analysis. For the predator-mediated apparent competition model (1.3) with one predator and two prey, a natural question is whether the system (1.3) can induce the Turing instability. In other words, can the one predator-prey system be destabilized by the invasion of another prey species? We shall attempt this question by starting with linear stability analysis.

4.1 Stability/instability of the non-spatial (ODE) system

We begin with the local/global stability of equilibria of the non-spatial system (1.2) with (1.4) or (1.5). For biological interest, the initial biomass of each species is assumed to be positive, namely $u(0), v(0), w(0) \geq 0$ ($\not\equiv 0$). We first recall the following stability results for the equilibria E_0, E_u, E_v and E_{uv} (cf. Lou et al. 2025)

Proposition 4.1 *For the non-spatial system (1.2) with either (1.4) or (1.5), the equilibria E_0, E_u and E_v are saddles, E_{uv} is a saddle if $\theta < L$, and E_{uv} is globally asymptotically stable if $\theta \geq L$.*

Table 2 The stability of equilibria of the ODE system (1.2) with (1.4)

	$\theta \in (0, \theta_0]$	$\theta \in (\theta_0, L)$	$\theta \in [L, \infty)$
$\alpha_1 > \alpha_2$	P_2 is GAS	$2P_*$is GAS	E_{uv} is GAS
$\alpha_1 < \alpha_2$	P_1 is GAS	P_* is GAS	E_{uv} is GAS
$\alpha_1 = \alpha_2$ ($\Longleftrightarrow \theta_0 = 0$)		P_* is GAS	E_{uv} is GAS

Note: The abbreviation "GAS" stands for "globally asymptotically stable". The notation "$\Longleftrightarrow$" denotes "if and only if"

Table 3 The stability of equilibria of the ODE system (1.2) with (1.5)

$i \in \{1, 2\}$	$\theta \in (0, L_i)$	$\theta \in [L_i, L)$	$\theta \in [L, \infty)$
$(K_1, K_2) \in \Lambda_i$	Q_i is GAS	Unclear	E_{uv} is GAS
$(K_1, K_2) \in \Lambda_*$	Q_* is GAS	Q_* is GAS	E_{uv} is GAS
$(K_1, K_2) \notin \Lambda_1 \cup \Lambda_2 \cup \Lambda_*$	Unclear	Unclear	E_{uv} is GAS

Note: Here, $\Lambda_1 := \{(K_1, K_2) \mid K_1 \le \lambda_1 + u_{Q_1}, \frac{K_2}{f_2(K_2)} \le w_{Q_1}\}$, $\Lambda_2 := \{(K_1, K_2) \mid K_2 \le \lambda_2 + v_{Q_2}, \frac{K_1}{f_1(K_1)} \le w_{Q_2}\}$, and Λ_* is defined by (2.3). The abbreviation "GAS" stands for "globally asymptotically stable"

4.1.1 Non-spatial system with the Holling type I functional response

Let $f_1(u)$ and $f_2(v)$ be given by (1.4). Then the global stability of solutions to (1.2) can be classified completely, as shown in Table 2.

4.1.2 Non-spatial system with the Holling type II functional response

Unlike the Holling type I, the global dynamics of (1.2) with the Holloing type II functional response (1.5) can only be partially confirmed as shown in Table 3 for E_{uv}, Q_1, Q_2 and Q_* (cf. Lou et al. 2025).

As observed in Table 3, there are some parameter gaps where the global dynamics of the system (1.2) with (1.5) remain ambiguous. Indeed it is too complicated to derive affirmative results in these gaps for general parameters. Mediated by a shared predator species, apparent competition between two prey species may be symmetric or asymmetric (see (Holt and Bonsall 2017, Figure 1)), where symmetric (resp. asymmetric) apparent competition occurs when two prey species have the same (resp. different) ecological characteristics. For clarity and definiteness, the stability analysis was conducted in Lou et al. (2025) to explore the effect of the predator-mediated apparent competition on population dynamics in two specific parameter configurations characterizing symmetric and asymmetric apparent competition. Below we shall briefly recall these results to investigate the pattern formation driven by the dispersal strategies of species later.

- **Symmetric apparent competition.** With the parameter configuration

$$K_1 = K_2 = 3 \quad \text{and} \quad \beta_1 = \beta_2 = h_1 = h_2 = \gamma_1 = \gamma_2 = 1, \tag{4.1}$$

Table 4 Stability of the equilibria of the ODE system (1.2) with (1.5) and (4.1)

Equilibria	θ										
	$(0, \frac{1}{2})$	$\frac{1}{2}$	$(\frac{1}{2}, \frac{2}{3})$	$\frac{2}{3}$	$(\frac{2}{3}, \theta_1)$	$[\theta_1, \frac{3}{4})$	$[\frac{3}{4}, 1)$	1	$(1, \frac{4}{3})$	$[\frac{4}{3}, \frac{3}{2})$	$[\frac{3}{2}, \infty)$
E_0, E_u, E_v	Saddle	Saddle	Saddle	Saddle	Saddle	Saddle	Saddle	Saddle	Saddle	Saddle	Saddle
E_{uv}	Saddle	Saddle	Saddle	Saddle	Saddle	Saddle	Saddle	Saddle	Saddle	Saddle	GAS
Q_1, Q_2	SF	MS	S-FN	MS	SF	Saddle	/	/	/	/	/
Q_*^0	U-FN	U-FN	U-FN	U-FN	U-FN	U-FN	U-FN	MS	S-FN	GAS	/
Q_*^1, Q_*^2	/	/	/	/	S-FN	S-FN	S-FN	/	/	/	/

Note: The abbreviations "SF", "MS", "S-FN", "U-FN" and "GAS" stand for "saddle-focus", "marginally stable", "stable focus node", "unstable focus node" and "globally asymptotically stable", respectively. The notation "/" denotes "equilibria do not exist"

it follows that $L_1 = L_2 = \frac{3}{4}$ and $L = \frac{3}{2}$. The system (1.2) with (1.5) and (4.1) has the equilibria

$$\begin{cases} E_0, E_u, E_v, E_{uv}, Q_1, Q_2, Q_*^0, & \text{if } \theta \in (0, \frac{2}{3}], \\ E_0, E_u, E_v, E_{uv}, Q_1, Q_2, Q_*^0, Q_*^1, Q_*^2, & \text{if } \theta \in (\frac{2}{3}, \frac{3}{4}), \\ E_0, E_u, E_v, E_{uv}, Q_*^0, Q_*^1, Q_*^2, & \text{if } \theta \in [\frac{3}{4}, 1), \\ E_0, E_u, E_v, E_{uv}, Q_*^0, & \text{if } \theta \in [1, \frac{3}{2}), \\ E_0, E_u, E_v, E_{uv}, & \text{if } \theta \in [\frac{3}{2}, \infty), \end{cases} \tag{4.2}$$

where $E_0 = (0, 0, 0)$, $E_u = (3, 0, 0)$, $E_v = (0, 3, 0)$, $E_{uv} = (3, 3, 0)$, and

$$\begin{cases} Q_1 = \left(\frac{\theta}{1-\theta}, 0, \frac{3-4\theta}{3(1-\theta)^2}\right), \quad Q_2 = \left(0, \frac{\theta}{1-\theta}, \frac{3-4\theta}{3(1-\theta)^2}\right), \\ Q_*^0 = \left(\frac{\theta}{2-\theta}, \frac{\theta}{2-\theta}, \frac{4(3-2\theta)}{3(2-\theta)^2}\right), \\ Q_*^1 = \left(1 + 2\sqrt{\frac{1-\theta}{2-\theta}}, 1 - 2\sqrt{\frac{1-\theta}{2-\theta}}, \frac{4}{3(2-\theta)}\right), \ Q_*^2 = \left(1 - 2\sqrt{\frac{1-\theta}{2-\theta}}, 1 + 2\sqrt{\frac{1-\theta}{2-\theta}}, \frac{4}{3(2-\theta)}\right). \end{cases} \tag{4.3}$$

The stability results of the above equilibria are summarized in Table 4.

- **Asymmetric apparent competition.** In this case, the parameter configuration is taken as

$$K_1 = K_2 = h_1 = h_2 = 1, \ \beta_1 = \beta_2 = b > 0 \quad \text{and} \quad 0 < \gamma_2 < \gamma_1 = 1. \tag{4.4}$$

Then $L_1 = \frac{b}{2} > L_2 = \frac{b\gamma_2}{1+\gamma_2}$, $L = \frac{b(1+3r_2)}{2(1+r_2)}$, and system (1.2) with (1.5) and (4.4) has the equilibria

Table 5 Stability of equilibria of the ODE system (1.2) with (1.5) and (4.4)

θ	$(0, \theta_*]$	(θ_*, L)	$[L, \infty)$
Global stability	Q_2 is GAS	Q_* is GAS	E_{uv} is GAS

Note: The abbreviation "GAS" stands for "globally asymptotically stable"

$$\begin{cases} E_0, E_u, E_v, E_{uv}, Q_1, Q_2, & \text{if } \theta \in (0, \theta_*], \\ E_0, E_u, E_v, E_{uv}, Q_1, Q_2, Q_*, & \text{if } \theta \in (\theta_*, L_2), \\ E_0, E_u, E_v, E_{uv}, Q_1, Q_*, & \text{if } \theta \in [L_2, L_1), \\ E_0, E_u, E_v, E_{uv}, Q_*, & \text{if } \theta \in [L_1, L), \\ E_0, E_u, E_v, E_{uv}, & \text{if } \theta \in [L, \infty), \end{cases}$$

where $E_0 = (0, 0, 0)$, $E_u = (1, 0, 0)$, $E_v = (0, 1, 0)$, $E_{uv} = (1, 1, 0)$,

$$Q_1 = \left(\frac{\theta}{b - \theta}, 0, \frac{b(b - 2\theta)}{(b - \theta)^2} \right),$$
$$Q_2 = \left(0, \frac{\theta}{\gamma_2(b - \theta)}, \frac{b(b\gamma_2 - (1 + \gamma_2)\theta)}{\gamma_2^2(b - \theta)^2} \right),$$

and

$$\theta_* = \varphi_1(\gamma_2) b \in (0, L_2),$$
$$\varphi_1(\gamma_2) := \frac{\sqrt{(1 - \gamma_2)(3\gamma_2 + 1)} - (1 - \gamma_2)(2\gamma_2 + 1)}{2\gamma_2^2} \in (0, \frac{1}{4}].$$

The (unique) coexistence equilibrium Q_* exists if and only if $\theta \in (\theta_*, L)$ (cf. (Lou et al. 2025, Appendix B)). In this case, the global population dynamics can be completely understood (see Lou et al. 2025), as shown in Table 5.

4.2 Stability and instability of the spatial (PDE) system

We next consider the system (1.3) with (1.4) or (1.5). When the spatial dimension $n \leq 2$, Theorem 2.2(ii), Theorem 2.3(ii) and Remark 2.1 imply that for $\theta \geq L$, E_{uv} remains globally asymptotically stable under spatial perturbations. This along with Proposition 4.1 shows that possible Turing instability can only arise from the constant semi-coexistence/coexistence steady states. We begin with the following general framework of linear stability analysis, where the spatial dimension $n \geq 1$ (note that the linear stability analysis does not require global boundedness).

4.2.1 General linear stability analysis

Linearize the system (1.3) at a constant steady state $E_s = (u_s, v_s, w_s)$ to get

$$\begin{cases} \Psi_t = \mathcal{M}\Delta\Psi + \mathcal{J}\Psi, & x \in \Omega, t > 0, \\ \partial_\nu \Psi = 0, & x \in \partial\Omega, t > 0, \\ \Psi(x,0) = (u_0 - u_s, v_0 - v_s, w_0 - w_s)^{\mathcal{T}}, & x \in \Omega, \end{cases} \tag{4.5}$$

where $\Psi(x,t) = (u - u_s, v - v_s, w - w_s)^{\mathcal{T}}$ and $\partial_\nu \Psi(x,t) = (\partial_\nu u, \partial_\nu v, \partial_\nu w)^{\mathcal{T}}$ with $\mathcal{T}$ denoting the transpose, and the matrices $\mathcal{M} = \mathcal{M}(E_s)$ and $\mathcal{J} = \mathcal{J}(E_s)$ are given by

$$\mathcal{M} := \begin{pmatrix} d_1 & 0 & 0 \\ 0 & d_2 & 0 \\ -\chi_1 w_s & -\chi_2 w_s & d_3 \end{pmatrix}, \ \mathcal{J} := \begin{pmatrix} J_{11} & J_{12} & J_{13} \\ J_{21} & J_{22} & J_{23} \\ J_{31} & J_{32} & J_{33} \end{pmatrix} \tag{4.6}$$

with

$$\begin{pmatrix} J_{11} & J_{12} & J_{13} \\ J_{21} & J_{22} & J_{23} \\ J_{31} & J_{32} & J_{33} \end{pmatrix} = \begin{pmatrix} 1 - \frac{2u_s}{K_1} - w_s f_1'(u_s) & 0 & -f_1(u_s) \\ 0 & 1 - \frac{2v_s}{K_2} - w_s f_2'(v_s) & -f_2(v_s) \\ \beta_1 w_s f_1'(u_s) & \beta_2 w_s f_2'(v_s) & \beta_1 f_1(u_s) + \beta_2 f_2(v_s) - \theta \end{pmatrix}.$$

By the separation of variables, we know that the linear system (4.5) has the solution in the form of

$$\Psi(x,t) = \sum_{k \geq 0} (U_k, V_k, W_k)^{\mathcal{T}} e^{\rho_k t} \zeta_k(x).$$

Here ρ_k is the temporal eigenvalue, $(U_k, V_k, W_k)^{\mathcal{T}}$ are the coefficients of the Fourier expansion of the initial function $\Psi(x,0)$ in terms of $\zeta_k(x)$ which are eigenfunctions of the eigenvalue problem

$$\begin{cases} -\Delta\zeta_k(x) = \mu_k \zeta_k(x), & x \in \Omega, \\ \partial_\nu \zeta_k(x) = 0, & x \in \partial\Omega, \end{cases} \tag{4.7}$$

where $\{\mu_k\}_{k \geq 0}$ denote the eigenvalues of $-\Delta$ under the Neumann boundary condition with $0 = \mu_0 < \mu_1 \leq \mu_2 \leq \mu_3 \leq \ldots$. Substituting (4.7) into (4.5), we arrive at

$$\rho_k \zeta_k(x) = -\mu_k \mathcal{M}\zeta_k(x) + \mathcal{J}\zeta_k(x) = \mathcal{B}\zeta_k(x),$$

with the matrix $\mathcal{B}$ given by

$$\mathcal{B} := -\mu_k \mathcal{M} + \mathcal{J} = \begin{pmatrix} -d_1\mu_k + J_{11} & 0 & J_{13} \\ 0 & -d_2\mu_k + J_{22} & J_{23} \\ \chi_1 w_s \mu_k + J_{31} & \chi_2 w_s \mu_k + J_{32} & -d_3\mu_k + J_{33} \end{pmatrix}.$$

Using (4.6) and denoting the three eigenvalue of $\mathcal{B}$ by ρ_k^0 and $\rho_k^{\pm}$, we know that ρ_k^0 and $\rho_k^{\pm}$ are the roots of

$$\varphi(\rho_k) := \rho_k^3 + A_2\rho_k^2 + A_1\rho_k + A_0 = 0, \tag{4.8}$$

where

$$\begin{cases} A_2 := D_2\mu_k - tr(\mathcal{J}), \\ A_1 := D_1\mu_k^2 - (Y_1 + X_1)\,\mu_k + Y_2, \\ A_0 := D_0\mu_k^3 - (Y_3 + X_2)\,\mu_k^2 + (Y_4 + X_3)\,\mu_k - Det(\mathcal{J}), \end{cases} \tag{4.9}$$

with

$$\begin{cases} D_2 = d_1 + d_2 + d_3 > 0, \quad D_1 = d_1d_2 + d_1d_3 + d_2d_3 > 0, \quad D_0 = d_1d_2d_3 > 0, \\ tr(\mathcal{J}) := J_{11} + J_{22} + J_{33}, \quad Det(\mathcal{J}) := J_{11}J_{22}J_{33} - J_{11}J_{23}J_{32} - J_{13}J_{22}J_{31}, \\ Y_1 := d_1\,(J_{22} + J_{33}) + d_2\,(J_{11} + J_{33}) + d_3\,(J_{11} + J_{22})\,, \\ Y_2 := J_{11}J_{22} + J_{11}J_{33} + J_{22}J_{33} - J_{13}J_{31} - J_{23}J_{32}, \\ Y_3 := d_1d_2J_{33} + d_1d_3J_{22} + d_2d_3J_{11}, \\ Y_4 := d_1\,(J_{22}J_{33} - J_{23}J_{32}) + d_2\,(J_{11}J_{33} - J_{13}J_{31}) + d_3J_{11}J_{22}, \\ X_1 := (\chi_1J_{13} + \chi_2J_{23})\,w_s, \quad X_2 := (d_2\chi_1J_{13} + d_1\chi_2J_{23})\,w_s, \\ X_3 := (\chi_1J_{13}J_{22} + \chi_2J_{11}J_{23})\,w_s. \end{cases} \tag{4.10}$$

It follows from the Routh-Hurwitz criterion (cf. (Murray 2002, Appendix B)) that all roots of (4.8) have negative real parts if and only if

$$A_2, A_1, A_0 > 0 \quad \text{and} \quad A_* := A_1A_2 - A_0 = D_3\mu_k^3 + B_4\mu_k^2 + B_2\mu_k + B_0 > 0, \tag{4.11}$$

where

$$\begin{cases} D_3 := D_1D_2 - D_0 = (d_1 + d_2)(d_1 + d_3)(d_2 + d_3) > 0, \\ B_4 := X_2 + Y_3 - D_2(X_1 + Y_1) - tr(\mathcal{J})D_1, \\ B_2 := tr(\mathcal{J})(X_1 + Y_1) + D_2Y_2 - X_3 - Y_4, \\ B_0 := Det(\mathcal{J}) - tr(\mathcal{J})Y_2. \end{cases} \tag{4.12}$$

The following discussion is divided into two parts for Holling type I and II functional responses, respectively.

4.2.2 Spatial system with the Holling type I functional response

Let $f_1(u)$ and $f_2(v)$ be given by (1.4). In view of Table 2, we aim to explore whether there is Turing instability arising from P_1, P_2, and P_* of the system (1.3). We first consider the linear stability of P_1 (resp. P_2) for $\theta \in (0, \theta_0]$ and $\alpha_1 < \alpha_2$ (resp. $\alpha_1 > \alpha_2$).

Lemma 4.2 *Let $f_1(u)$ and $f_2(v)$ be given by (1.4), and let $d_i > 0$ and $\chi_i \geq 0$. If $\theta \in (0, \theta_0]$ and $\alpha_1 < \alpha_2$ (resp. $\alpha_1 > \alpha_2$), then P_1 (resp. P_2) of system (1.3) is linearly stable.*

Proof We only prove for P_1, and the case of P_2 can be proved similarly. Let $E_s = P_1 = \left(\frac{\theta}{\alpha_1\beta_1}, 0, \frac{L_1-\theta}{\alpha_1 L_1}\right)$ in Sect. 4.2.1. Then we obtain that the eigenvalues of the matrix $\mathcal{B}$ are

$$\rho_k^0 = -d_2\mu_k + \frac{\alpha_2(\theta-\theta_0)}{\alpha_1 L_1} \quad \text{and} \quad \rho_k^{\pm} = -\frac{1}{2L_1}\left[(L_1(d_1+d_3)\mu_k + \theta) \pm \sqrt{I_3}\right],$$

where $I_3 := (d_1-d_3)^2 L_1^2\mu_k^2 + 2\theta\left[(d_1-d_3)L_1 + 2\chi_1 K_1(\theta - L_1)\right]\mu_k + [4L_1(\theta - L_1) + \theta]\theta$. For Turing instability, we only concern $\mu_k > 0$. Clearly, $\rho_k^0 \leq -d_2\mu_k < 0$ for $\theta \in (0, \theta_0]$. Moreover, if $I_3 \leq 0$, then $\mathrm{Re}(\rho_k^{\pm}) < 0$; if $I_3 > 0$, it also holds that $\mathrm{Re}(\rho_k^{\pm}) < 0$ since $0 < \theta \leq \theta_0 = \left(1 - \frac{\alpha_1}{\alpha_2}\right) L_1 < L_1$ and

$$\begin{aligned}(L_1(d_1+d_3)\mu_k + \theta)^2 - I_3 &= 4d_1d_3L_1^2\mu_k^2 + 4\theta\left[d_3L_1 + \chi_1K_1(L_1-\theta)\right]\mu_k \\ &\quad + 4L_1\theta(L_1-\theta) \\ &\geq 4L_1\theta(L_1-\theta) > 0.\end{aligned}$$

This completes the proof. □

We then consider the linear stability of P_* for $\theta \in (\theta_0, L)$.

Lemma 4.3 *Let $f_1(u)$ and $f_2(v)$ be given by (1.4), and let $d_i > 0$ and $\chi_i \geq 0$. If $\theta \in (\theta_0, L)$, then the unique positive constant steady state P_* of the system (1.3) is linearly stable.*

Proof Let $E_s = P_* = (u_*, v_*, w_*)$ in Sect. 4.2.1. Then (4.6) implies

$$\mathcal{J} = \begin{pmatrix} -\frac{u_*}{K_1} & 0 & -\alpha_1 u_* \\ 0 & -\frac{v_*}{K_2} & -\alpha_2 v_* \\ \alpha_1\beta_1 w_* & \alpha_2\beta_2 w_* & 0 \end{pmatrix}. \tag{4.13}$$

Therefore, we have from (4.10) that

$$-tr(\mathcal{J}),\ -(Y_1+X_1),\ Y_2,\ -(Y_3+X_2),\ (Y_4+X_3),\ -Det(\mathcal{J}) > 0,$$

which alongside (4.9) implies $A_2, A_1, A_0 > 0$. For $A_* = A_1A_2 - A_0 = D_3\mu_k^3 + B_4\mu_k^2 + B_2\mu_k + B_0$ given by (4.11), we have from (4.10), (4.12) and (4.13) that

$$\begin{aligned}B_4 &> X_2 + Y_3 - D_2(X_1+Y_1) \\ &= \frac{(D_1 + d_2^2 + d_3^2)u_*}{K_1} + \frac{(D_1 + d_1^2 + d_3^2)v_*}{K_2} \\ &\quad + \alpha_1(d_1+d_3)u_*w_*\chi_1 + \alpha_2(d_2+d_3)v_*w_*\chi_2 > 0,\end{aligned}$$

$$B_2 = \frac{(d_1+d_2)u_*v_* + \alpha_1 K_2 u_*^2 w_* \chi_1 + \alpha_2 K_1 v_*^2 w_* \chi_2}{K_1 K_2} + \left[\alpha_1^2 \beta_1 u_*(d_1+d_3) + \alpha_2^2 \beta_2 v_*(d_2+d_3)\right] w_* > 0,$$

$$B_0 = \frac{w_*\left(\alpha_1^2 \beta_1 K_2 u_*^2 + \alpha_2^2 \beta_2 K_1 v_*^2\right)}{K_1 K_2} + \frac{u_* v_*(K_1 v_* + K_2 u_*)}{K_1^2 K_2^2} > 0.$$

Therefore, $A_* = A_1 A_2 - A_0 > 0$. Now (4.11) is satisfied and the proof is completed. □

Remark 4.1 The above analysis indicates that the system (1.3) with the Holling type I functional response (1.4) has no Turing instability.

4.2.3 Spatial system with the Holling type II functional response

Let $f_1(u)$ and $f_2(v)$ be given by (1.5). Then we investigate whether system (1.3) admits Turing instability arising from Q_1, Q_2, and Q_* for the symmetric parameter configuration (4.1) and the asymmetric one (4.4) with general spatial dispersal coefficients

$$d_1, d_2, d_3 > 0 \quad \text{and} \quad \chi_1, \chi_2 \geq 0. \tag{4.14}$$

Below we shall focus on the symmetric parameter configuration (4.1), and give some brief remarks for the asymmetric one (4.4). Given the results in Table 4, we need to examine the linear stability of the following constant steady states: Q_1 and Q_2 for $\theta \in [\frac{1}{2}, \frac{2}{3}]$; Q_*^0 for $\theta \in [1, \frac{3}{2})$; Q_*^1 and Q_*^2 for $\theta \in (\frac{2}{3}, 1)$.

Lemma 4.4 *Let $f_1(u)$ and $f_2(v)$ be given by (1.5), and let (4.1) and (4.14) hold. Then the following results hold.*

(i) The semi-coexistence constant steady states Q_1 and Q_2 of the system (1.3) are marginally stable for $\theta = \frac{1}{2}, \frac{2}{3}$, and linearly stable for $\theta \in \left(\frac{1}{2}, \frac{2}{3}\right)$.

(ii) The positive constant steady state Q_*^0 is marginally stable for $\theta = 1$, and linearly stable for $\theta \in \left(1, \frac{3}{2}\right)$.

Proof The proof is similar to that of Lemmas 4.2 and 4.3 and is omitted for brevity. □

Lemma 4.4 show that there is no Turing instability arising from Q_1, Q_2 and Q_*^0. We shall see below that Turing instability may arise from Q_*^1 and Q_*^2. Since the two positive constant steady states Q_*^1 and Q_*^2 are symmetric in the first two components and the third component is the same, we only conduct stability analysis for Q_*^1, and the case for Q_*^2 is similar.

Instability arising from Q_*^1. In view of (4.2), Q_*^1 exists if and only if $\theta \in (\frac{2}{3}, 1)$. To avoid excessive technicalities, we let $\theta = \frac{7}{8} \in (\frac{2}{3}, 1)$. Then with the symmetric parameters in (4.1), we consider

$$\theta = \frac{7}{8},\ d_1, d_2, d_3 > 0,\ \chi_i \geq 0,\ K_i = 3,\ \beta_i = h_i = \gamma_i = 1, \quad i = 1, 2, \tag{4.15}$$

which implies

$$Q_*^1 = \left(\frac{5}{3}, \frac{1}{3}, \frac{32}{27}\right).$$

Let $E_s = Q_*^1$ in Sect. 4.2.1. Using (4.9), (4.11) and (4.15), we have

$$\begin{cases} A_2 = D_2\mu_k + \frac{1}{6} > 0, \\ A_1 = D_1\mu_k^2 + \left(\frac{-2d_1+5d_2+3d_3}{18} + \frac{20\chi_1+8\chi_2}{27}\right)\mu_k + \frac{311}{1296}, \\ A_0 = D_0\mu_k^3 + \left(\frac{(-2d_1+5d_2)d_3}{18} + \frac{20d_2\chi_1+8d_1\chi_2}{27}\right)\mu_k^2 \\ \qquad + \left(\frac{d_1}{6} + \frac{5d_2}{48} - \frac{5d_3}{162} + \frac{20(-\chi_1+\chi_2)}{243}\right)\mu_k + \frac{5}{144}, \\ A_* = D_3\mu_k^3 + \left(\frac{-2d_1^2+5d_2^2+3d_3^2+6D_1}{18} + \frac{20(d_1+d_3)\chi_1+8(d_2+d_3)\chi_2}{27}\right)\mu_k^2 \\ \qquad + \left(\frac{71d_1+236d_2+387d_3}{1296} + \frac{50\chi_1-8\chi_2}{243}\right)\mu_k + \frac{41}{7776}. \end{cases} \tag{4.16}$$

Then we have the following result from (4.11) immediately.

Lemma 4.5 *Let $f_1(u)$ and $f_2(v)$ be given by (1.5). With the parameter configuration (4.15), the following stability results hold for the positive constant steady state Q_*^1 of (1.3).*

(i) Q_*^1 is linearly stable if and only if $\min\limits_{\mu_k>0}\{A_0, A_1, A_*\} > 0$.

(ii) Turing instability will arise from Q_*^1 if and only if

$$\min_{\mu_k>0}\{A_0, A_1, A_*\} < 0. \tag{4.17}$$

Remark 4.2 It can be seen from (4.16) that there are many values of $(d, d_3, \chi_1, \chi_2) \in (0,\infty)^2 \times [0,\infty)^2$ such that (4.17) holds. Moreover, any of $\min\limits_{\mu_k>0} A_0$, $\min\limits_{\mu_k>0} A_1$ and $\min\limits_{\mu_k>0} A_*$ may be negative. Moreover, Turing patterns can be driven by pure diffusion (i.e., $\chi_1 = \chi_2 = 0$), which will be discussed in detail in Section 5.2.1.

Remark 4.3 The system (1.3) with the Holling type II functional response (1.5) and the symmetric parameter values in (4.15) has no Turing instability arising from Q_1, Q_2 and Q_*^0, but may induce Turing instability from Q_*^1 and Q_*^2 by diffusion or prey-taxis (see Lemma 4.5 and Remark 4.2). For the asymmetric parameters given in (4.4), Table 5 shows that the system (1.3) will globally asymptotically stabilize to Q_2, Q_* or E_{uv} depending on the value of θ. With spatial movements (diffusion and prey-taxis), stability analysis shows that Q_2, Q_* or E_{uv} are still linearly stable (omitted here for brevity) and hence no spatial patterns can bifurcate from Q_2, Q_* or E_{uv}.

5 Numerical simulations and spatiotemporal patterns

Remark 4.1 indicates that for the Holling type I functional response (1.4), the system (1.3) cannot generate Turing patterns. However, the pattern is possible with the Holling type II functional response (1.5) if the apparent competition is asymmetric (see Remark 4.3). In this section, we use numerical simulations to illustrate spatiotemporal patterns generated by the system (1.3) with the Holling type II functional response (1.5) and investigate the effects of spatial movement on the global population dynamics.

5.1 Onset of predator-mediated apparent competition

From our previous work (Lou et al., 2025), it is demonstrated that the predator-mediated apparent competition in the absence of spatial components is not necessarily effective since the invasive prey species may not successfully invade. Hence the first question concerned is whether the spatial movement (diffusion and/or prey-taxis) can impact the success/failure of invasion. Therefore, we need to examine the stability of the semi-coexistence constant steady state $Q_1 = (\frac{\theta}{1-\theta}, 0, \frac{3-4\theta}{3(1-\theta)^2})$ given by (4.3). Sect. 5 shows that for all $\theta > 0$ and spatial coefficients $(d_1, d_2, d_3, \chi_1, \chi_2) \in (0, \infty)^3 \times [0, \infty)^2$, Q_1 is linearly stable for the system (1.3) with (1.5). We shall perform numerical simulations to see the possible patterns. Without loss of generality, we let $\Omega = (0, 30\pi)$ and $\theta = \frac{1}{4}$, which gives $Q_1 = (\frac{1}{3}, 0, \frac{32}{27})$. For definiteness, we set $d_1 = d_2 = d_3 = 1$ and set the initial data as

$$(u_0, v_0, w_0) = Q_1 + (0, R + 0.01 \cdot \cos(\pi x), 0), \quad x \in \Omega, \tag{5.1}$$

where $R > 0$ represents the biomass of the invasive prey species to be chosen later. Now we study the effect of prey-taxis on predator-mediated apparent competition. We mainly discuss two cases: $(\chi_1, \chi_2) = (2, 1)$ and $(\chi_1, \chi_2) = (10, 1)$.

With $(\chi_1, \chi_2) = (2, 1)$, which indicates that the strength of prey-taxis on the native prey species is "slightly" stronger than that on the invasive prey species, we observe the following two prominent phenomena from the numerical simulations shown in Fig. 1.

(1) The initial biomass of invasive prey species plays a key role in determining the success/failure of invasions: small invasion biomass leads to failed invasions; medium and large invasion biomass leads to successful invasions and the native prey species are wiped out.
(2) The spatially homogeneous time-periodic patterns always asymptotically appear regardless of whether the invasion is successful or not. This implies that the long-time population dynamics are mainly dominated by the corresponding ODE (non-spatial) system and the spatial effect is negligible in the long run.

For $(\chi_1, \chi_2) = (10, 1)$, namely the strength of prey-taxis for the native prey species is much stronger than that for the invasive prey species, the numerical simulations are shown in Fig. 2, where the following phenomena can be found.

(i) The biomass of the invasive prey species is still a key factor determining whether the invasion is successful, same as in the former case $(\chi_1, \chi_2) = (2, 1)$.

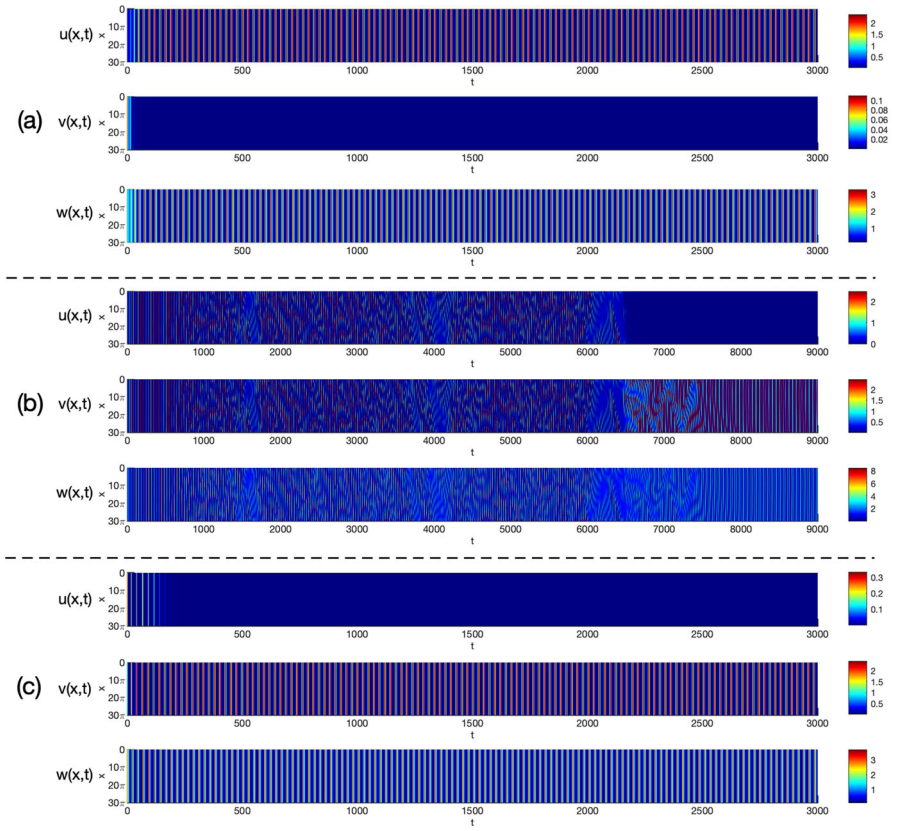

Fig. 1 Numerical simulations for the system (1.3) with (1.5) in the interval $\Omega = (0, 30\pi)$, under the parameter setting (4.1), $\theta = \frac{1}{4}$, $d_1 = d_2 = d_3 = 1$ and $(\chi_1, \chi_2) = (2, 1)$. The initial data are given by (5.1) with $R = 0.1$ in **(a)**, $R = 0.36$ in **(b)**, and $R = 1$ in **(c)**

(ii) Prey-taxis can induce spatially inhomogeneous patterns, see Fig. 2(a).

5.2 Instability driven by diffusion or prey-taxis

Based on the analyses in Sect. 5, we know that the system (1.3) with the Holling type I functional response (1.4) has no Turing instability. For the system (1.3) with the Holling type II functional response (1.5), Lemma 4.5(ii) shows that the instability of Q_*^1 may be driven by diffusion and/or prey-taxis in the case of symmetric apparent competition with parameter configuration (4.15). Next we shall show that the sole diffusion-drive instability is possible without prey-taxis (i.e. $\chi_1 = \chi_2 = 0$), and further investigate the influence of prey-taxis on the pattern formation.

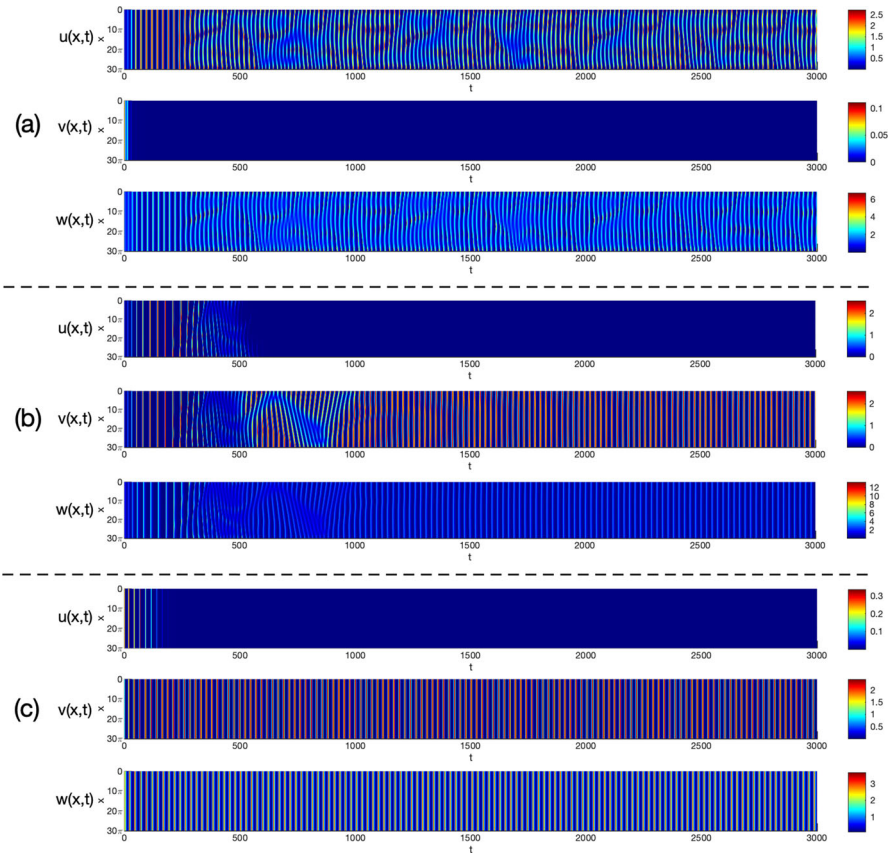

Fig. 2 Numerical simulations for the system (1.3) with (1.5) in the interval $\Omega = (0, 30\pi)$, under the parameter setting (4.1), $\theta = \frac{1}{4}$, $d_1 = d_2 = d_3 = 1$ and $(\chi_1, \chi_2) = (10, 1)$. The initial data are given by (5.1) with $R = 0.1$ in **(a)**, $R = 0.36$ in **(b)**, and $R = 1$ in **(c)**

5.2.1 Diffusion-driven instability

With Lemma 4.5 and (4.16), there are many values of $d_1, d_2, d_3 > 0$ with $\chi_1 = \chi_2 = 0$ which can satisfy (4.17) and hence give rise to Turing instability. We particularly consider three typical sets of diffusion rates as follows:

$$\begin{cases} \mathbf{E.1} : (d_1, d_2, d_3) = (1, 1, 60), \\ \mathbf{E.2} : (d_1, d_2, d_3) = (60, 1, 1), \\ \mathbf{E.3} : (d_1, d_2, d_3) = (60, \frac{1}{60}, 1). \end{cases} \tag{5.2}$$

It can be shown that system (1.3) with (1.5) and parameter setting given (4.15) and (5.2) may generate various bifurcations from Q^1_*, as summarized in Table 6.

Remark 5.1 It is known that the spatial one predator-one prey systems without prey-taxis do not have Turing instability (see Appendix A). However, in the system (1.3),

Table 6 Turing bifurcations arising from system (1.3) with (1.5), (4.15) and (5.2), where $\chi_1 = \chi_2 = 0$

(d_1, d_2, d_3)	**E.1**	**E.2**	**E.3**
$\min_{\mu_k>0} A_1$	+	+	+
$\min_{\mu_k>0} A_0$	−	+	−
$\min_{\mu_k>0} A_*$	+	−	−
Bifurcation	Steady-state bifurcation	Hopf bifurcation	Steady-state bifurcation and Hopf bifurcation

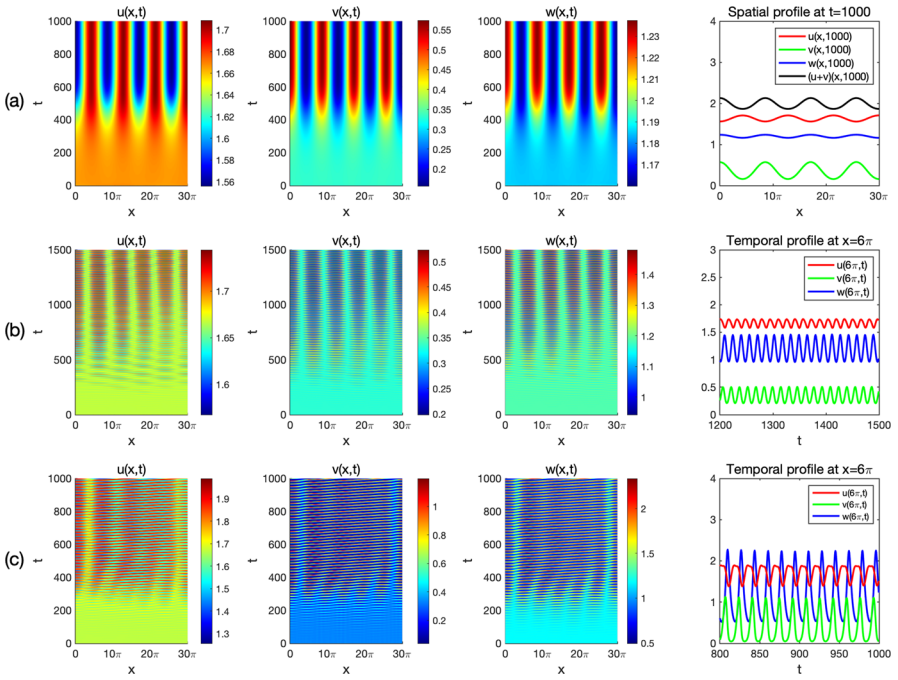

Fig. 3 Numerical simulations for the system (1.3) with (1.5) in the interval $\Omega = (0, 30\pi)$, under the parameters setting (4.15) with $\chi_1 = \chi_2 = 0$, for different values of (d_1, d_2, d_3) given in (5.2): **E.1** in row **(a)**, **E.2** in row **(b)**, and **E.3** in row **(c)**. The initial value is given as a small random perturbation of $Q_*^1 = \left(\frac{5}{3}, \frac{1}{3}, \frac{32}{27}\right)$

where two prey species have negative indirect interactions mediated by one shared predator, diffusion can induce various Turing bifurcations resulting in profound spatial or periodic patterns as illustrated in Fig. 3.

We next consider the role of prey-taxis. It turns out that the interactions between prey-taxis and diffusion are quite delicate. For given diffusion coefficients, different values of χ_1 and χ_2 may have different effects (stabilization or destabilization) as demonstrated below.

5.2.2 Prey-taxis driven instability

We now show the prey-taxis may destabilize the system (1.3) with (1.5). We shall choose $\chi_1, \chi_2 \geq 0$ as the bifurcation parameters to study the prey-taxis driven instability arising from Q_*^1. We assume the two prey species have the same diffusion rates, that is, $d_1 = d_2 = d > 0$. For the sake of presentation, we denote

$$\begin{aligned}
&\mathcal{S}_1 := \left\{ k \,\middle|\, 0 < \mu_k < \frac{1}{9d} \right\}, \ \mathcal{S}_2 := \left\{ k \,\middle|\, 0 < \mu_k < \frac{1}{9(d+d_3)} \right\}, \\
&\chi_1^* = \chi_1^*(\chi_2, d, d_3) := \min_{k \in \mathcal{S}_1} \left\{ \frac{I_4}{320\mu_k\,(1-9d\mu_k)} + \frac{(18d\mu_k+5)\chi_2}{5\,(1-9d\mu_k)} \right\}, \\
&\chi_2^* = \chi_2^*(\chi_1, d, d_3) := \min_{k \in \mathcal{S}_2} \left\{ \frac{5\chi_1\,(18\mu_k(d+d_3)+5)}{4\,(1-9\mu_k(d+d_3))} + \frac{I_5}{256\mu_k\,(1-9\mu_k(d+d_3))} \right\} > 0, \\
&I_4 := -24d_3\mu_k\,(1-9d\mu_k)\,(18d\mu_k+5) + 27\,(39d\mu_k+5)\,, \\
&I_5 := 1296\mu_k^2\left(3d^2+4dd_3+d_3^2\right) + 15552d\mu_k^3(d+d_3)^2 + 6\mu_k(307d+387d_3) + 41 > 0. \qquad (5.3)
\end{aligned}$$

Then we can make the conclusions of Lemma 4.5(ii) more specific as follows.

Lemma 5.1 *Let $f_1(u)$ and $f_2(v)$ be given by (1.5). For the parameter setting (4.15) with with $d_1 = d_2 = d > 0$, the positive equilibrium Q_*^1 of the system (1.3) is linearly unstable if and only if*

$$\text{either} \quad \min_{\mu_k>0} A_0 < 0 \quad \text{or} \quad \min_{\mu_k>0} A_* < 0. \qquad (5.4)$$

Moreover, the following results hold.

(a) The steady-state bifurcation occurs (i.e. $\min_{\mu_k>0} A_0 < 0$) if and only if

$$\mathcal{S}_1 \neq \emptyset \quad \text{and} \quad (\chi_1, \chi_2) \in \Omega_1 := \left\{ (\chi_1, \chi_2) \in [0,\infty)^2 \mid \chi_1 > \chi_1^*(\chi_2, d, d_3) \right\}.$$

(b) The Hopf bifurcation occurs (i.e. $\min_{\mu_k>0} A_* < 0$) if and only if

$$\mathcal{S}_2 \neq \emptyset \quad \text{and} \quad (\chi_1, \chi_2) \in \Omega_2 := \left\{ (\chi_1, \chi_2) \in [0,\infty)^2 \mid \chi_2 > \chi_2^*(\chi_1, d, d_3) \right\}.$$

Proof Clearly, (4.16) with $d_1 = d_2 = d > 0$ implies that $A_2, A_1 > 0$. Moreover, elementary analysis shows that

$$\max\left\{ \min_{\mu_k>0} A_0, \min_{\mu_k>0} A_* \right\} > 0 \quad \text{for all } d, d_3 > 0,\ \chi_1, \chi_2 \geq 0.$$

Therefore, Lemma 4.5 implies that Q_*^1 is linearly unstable if and only if (5.4) holds. The proofs for (a) and (b) are straightforward with tedious computations and we omit the details. □

In the absence of prey-taxis (i.e. $\chi_1 = \chi_2 = 0$), Lemma 5.1 indicates that the Hopf bifurcation can never occur due to $\chi_2^* > 0$, and (5.3) implies that the steady-state bifurcation occurs if and only if

$$d_3 > d_3^* := \min_{k\in\mathcal{S}_1} \phi_2(\mu_k, d), \quad \phi_2(\mu_k, d) := \frac{9\,(39d\mu_k + 5)}{8\mu_k\,(1 - 9d\mu_k)\,(18d\mu_k + 5)}. \tag{5.5}$$

It can be checked that $\frac{\partial\phi_2(\mu_k,d)}{\partial d} > 0$ for $0 < \mu_k < \frac{1}{9d}$. Without loss of generality, we let $d_1 = d_2 = d = 1$. Then

$$d_3^* = \min_{0<\mu_k<\frac{1}{9}} \phi_2\,(\mu_k, 1) \approx \phi_2\,(\mu_k, 1)\,|_{\mu_k\approx 0.0517} \approx 48.1461.$$

Remark 5.2 In an interval $\Omega = (0, \ell)$ with $\ell > 0$, the following conclusions can be drawn from Lemma 5.1.

(i) If $\ell \in (0, 3\pi]$, there is no Turing instability.
(ii) If $\ell \in (3\pi, 3\sqrt{1 + d_3}\pi]$, only the steady-state bifurcation can occur.
(iii) If $\ell > 3\sqrt{1 + d_3}\pi$, either the steady-state bifurcation or Hopf bifurcation may occur.

We still take $l = 30\pi$ so that two types of bifurcations may occur. Without prey-taxis ($\chi_1 = \chi_2 = 0$), (5.5) gives

$$d_3^* = \min_{0<\mu_k<\frac{1}{9}} \phi_2\,(\mu_k, 1) = \phi_2\left(\left(\frac{7\pi}{l}\right)^2, 1\right) \approx 48.2626.$$

Consider two typical cases:

$$d_3 = 1 < d_3^*, \quad d_3 = 60 > d_3^*,$$

where the former (resp. latter) implies Q_*^1 is linearly stable (resp. unstable) by Lemma 5.1. The numerical simulation for $d_3 = 60$ was already shown in Fig. 3(a). Then geometric illustration of the instability parameter regions Ω_1 and Ω_2 in the χ_1-χ_2 plane are shown in Fig. 4. Clearly, $\Omega_1 \cap \Omega_2 = \emptyset$ due to (5.4). Denoting

$$l_i := \left\{(\chi_1, \chi_2) \in [0, \infty)^2 \mid \chi_i = \chi_i^*(\chi_j, d, d_3)\right\},\ i + j = 3,\ i = 1, 2,$$

we can verify that the curve l_2 lies above l_1, as shown in Fig. 4. We denote the region bounded by $l_i (i = 1, 2)$ and $\chi_i (i = 1, 2)$ axes by Ω_3. Then Q_1^* is linearly stable and there is no pattern formation in Ω_3.

The above analyses indicate that prey-taxis can drive the instability of constant steady states of from system (1.3) with the Holling type II functional response (1.5) under certain parameter regions such as the parameter configuration given in (4.15)

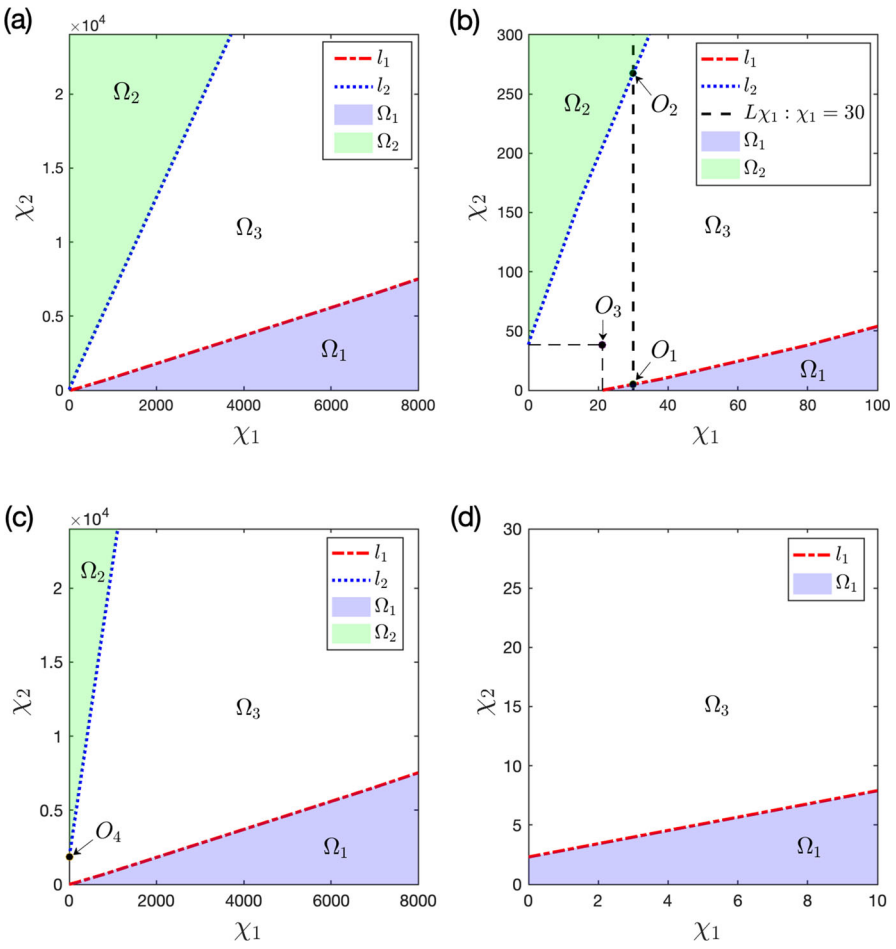

Fig. 4 Stability parameter regions Ω_i $(i = 1, 2, 3)$ in the χ_1-χ_2 plane for $d_1 = d_2 = 1$ and different values of d_3, with $d_3 = 1$ in **(a)-(b)** and $d_3 = 60$ in **(c)-(d)**, where figures in **(b)** and **(d)** are the amplified portions of **(a)** and **(c)** near the origin, respectively. The auxiliary line $L\chi_1$ in **(b)** intersects with l_1 and l_2 at the points $O_1 \approx (30, 4.9275)$ and $O_2 \approx (30, 267.3756)$, respectively, $O_3 \approx (21.1921, 38.34)$ and $O_4 \approx (0, 1839.6170)$

with $d_1 = d_2 = 1$. These instabilities may result in the steady-state or Hopf bifurcations. Next we perform numerical simulations to illustrate the possible emerging spatial patterns. To this end, we set the parameter values as

$$\theta = \frac{7}{8},\ d_1 = d_2 = d_3 = 1,\ K_i = 3,\ \beta_i = h_i = \gamma_i = 1,\quad i = 1, 2. \tag{5.6}$$

With parameters chosen in (5.6), we see that $d_3 = 1 < d_3^*$ and hence diffusion can not induce Turing instability if $\chi_1 = \chi_2 = 0$ (see the above discussions). Now we take the values of (χ_1, χ_2) on the vertical line $L\chi_1 : \chi_1 = 30$ in Fig. 4(b) and

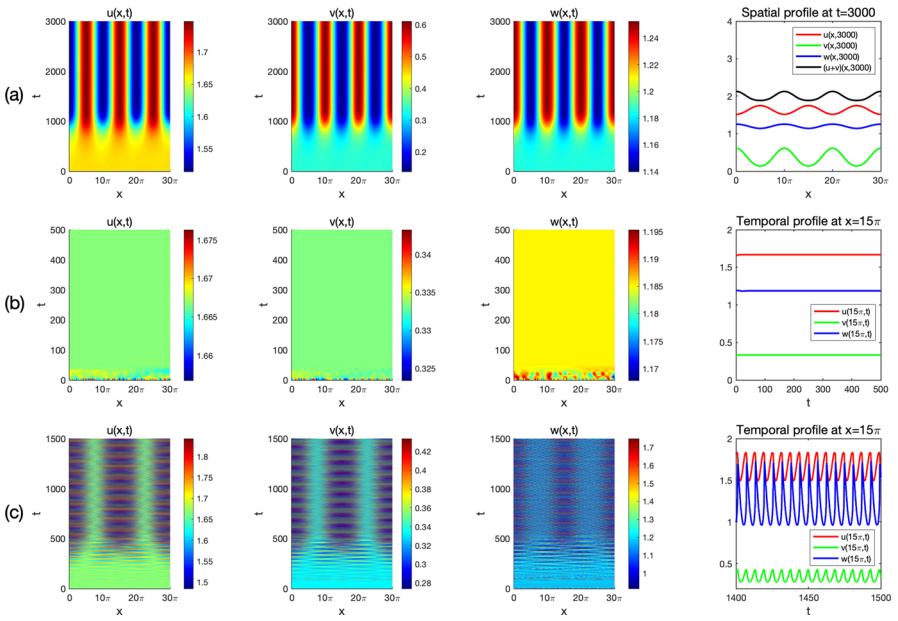

Fig. 5 Numerical simulations for the system (1.3) with (1.5) in the interval $\Omega = (0, 30\pi)$, under the parameter setting (5.6), $\chi_1 = 30$ and different values of χ_2: $\chi_2 = 3$ in **(a)**, $\chi_2 = 100$ in **(b)**, and $\chi_2 = 500$ in **(c)**. The initial value is chosen as a small random perturbation of $Q_*^1 = \left(\frac{5}{3}, \frac{1}{3}, \frac{32}{27}\right)$

$\chi_2 = 3, 6, 500$, where $(\chi_1 = 30, \chi_2 = 1) \in \Omega_1$, $(\chi_1 = 10, \chi_2 = 6) \in \Omega_3$ and $(\chi_1 = 30, \chi_2 = 500) \in \Omega_2$. For $\chi_2 = 3$, the steady-state bifurcation occurs, and the corresponding numerical simulations are shown in Fig. 5(a), where non-constant stable spatial patterns are observed. When χ_2 increases along the vertical line $L\chi_1$ in Fig. 4(b) and crosses the steady-state bifurcation boundary curve l_1 at the point O_1 into region Ω_3, then the solution of (1.3) stabilizes to the positive constant steady state Q_*^1. However, when χ_2 further increases along the vertical line $L\chi_1$ and crosses the Hopf bifurcation boundary curve l_2 at the point O_2 into the region Ω_2, the Hopf bifurcation will occur and patterns will arise from Q_*^1 as shown in Fig. 5(c) where we observe the temporally oscillatory and spatially inhomogeneous patterns. Therefore, fixing $\chi_1 > 0$, we see that only when χ_2 is small (i.e. below the curve l_1) or large (i.e. above the curve l_2), the instability can occur and spatial patterns arise. This is similar to $\chi_1 > 0$ by fixing $\chi_2 > 0$, see Fig. 4(a)-(b). However if $(\chi_1, \chi_2) \in \Omega_3$ (i.e. the values of χ_1 and χ_2 are moderate), there is no spatial patterns.

5.2.3 Prey-taxis driven stability

We still consider the three examples in (5.2) with parameter configuration (4.15). For these parameter values, the analysis in Sect. 5.2.1 says that Q_*^1 with $\chi_1 = \chi_2 = 0$ is linearly unstable, and hence spatial patterns will develop from Q_*^1 as shown in Fig. 3. Now we let $\chi_1, \chi_2 > 0$ and keep other parameter values the same. For definiteness, we fix $\chi_1 = \chi_2 = 10$ without loss of generality. Then it can be checked

that $\min_{\mu_k>0}\{A_0, A_1, A_*\} > 0$ (calculations are routine and omitted here for brevity), and hence Q_*^1 is linearly stable by Lemma 4.5. This implies that the prey-taxis plays a stabilization role in this case. To make this visulizable, we consider a specific example **E.1** in (5.2) with parameter values (4.15) by choosing $d_1 = d_2 = 1$ and $d_3 = 60$ and plot the instability/stability parameter regions in Fig. 4(c)-(d) where we see that the instability region Ω_1 contains the origin $(\chi_1, \chi_2) = (0, 0)$. If we increase the value of χ_2 so that (χ_1, χ_2) falls inside Ω_3, then Q_1^* becomes stable and spatial patterns may stabilize into the constant Q_1^* as demonstrated by the numerical simulations shown in Fig. 5(b).

Remark 5.3 The above analyses and results along with numerical simulations show that prey-taxis in the predator-mediated apparent competition system may play complex roles. For instance, if the parameter values are given by (4.15), we find that prey-taxis may induce the instability if (χ_1, χ_2) falls inside Ω_1 or Ω_2 while stability if $(\chi_1, \chi_2) \in \Omega_3$. This contrasts with one predator-one prey systems with prey-taxis which plays a single role, either stabilization (cf. Cai et al. 2022) or destabilization (cf. Song and Tang 2017). These observations along with the statement in Remark 5.1 assert that both diffusion and prey-taxis in one predator-two prey systems with the predator-mediated apparent competition can play significant roles different from the one predator-one prey systems. This implies that spatial movements will play more profound roles with the increasing number of species.

6 Summary and discussion

In our previous work (Lou et al., 2025), we considered a temporal system (i.e. ODE counterpart of (1.3)) to explore the effects and biological consequences of the predator-mediated apparent competition (i.e. two prey species have an indirect negative interaction mediated by a shared predator species). The local and global stability of the equilibria of the temporal system with Holling type I and II functional responses were established and numerical simulations were performed to demonstrate the population dynamics and biological consequences caused by the predator-mediated apparent competition. However, the spatial movement of species, which is an indispensable factor in applications, was not considered in Lou et al. (2025). The goal of this paper is to include diffusion and prey-taxis into the ODE (temporal) system, leading to the system (1.3), and explore the spatial effects on the population dynamics and distributional structures.

With Holling type I and II functional responses, we establish the global stability of the coexistence (i.e. positive) and the predator-free constant steady states in certain parameter regimes. This yields a threshold dynamics in terms of the predator's death rate, addressing under what conditions the spatial homogeneity can be achieved. Outside these parameter regimes, we conduct linear analysis to find the instability parameter regions by which we perform numerical simulations to demonstrate various intricate patterns arising from (1.3) with the Holling II functional response. With these numerical simulations, we find some interesting biological implications as summarized in (f.2)-(f.4) in Sect. 2.2. However, these implications are derived from numerical

simulations or local instability analysis. Hence how to mathematically justify these patterns (like existence or stability) remains an interesting question. In particular, we find that spatial movements, including diffusion and prey-taxis, in the predator-prey system with two prey species will have significantly different effects from the system with one prey species. This implies that the effect of spatial movements can be distinct in complex ecological predator-prey systems depending on the number of species, and hence suggests that oversimplified models may not be adequate to describe the complex behavior of real ecosystems. More complicated models, though mathematically challenging, are often useful to gain a deeper understanding of the complex dynamics of realistic ecological systems.

Appendix A. Stability of one predator-one prey systems with prey-taxis

This appendix is devoted to investigating whether there is Turing instability arising from the following one predator-one prey system with prey-taxis

$$\begin{cases} u_t = d_1\Delta u + u\,(1-u/K) - wf(u), & x\in\Omega,\ t>0,\\ w_t = d_2\Delta w - \chi\nabla\cdot(w\nabla u) + w\,(\beta f(u)-\theta)\,, & x\in\Omega,\ t>0,\\ \partial_\nu u = \partial_\nu w = 0, & x\in\partial\Omega,\ t>0, \end{cases} \tag{A1}$$

where $\Omega\subset\mathbb{R}^n$ ($n\geq 1$) is a bounded domain with smooth boundary, $\partial_\nu := \frac{\partial}{\partial\nu}$ and ν is the outward unit normal vector on $\partial\Omega$, u and w denote the densities of the prey and the predator species, respectively. The system (A1) is a special case of the system (1.3) without the invasive prey species. Parameters d_1 and d_2 are diffusion rates of the prey and the predator, respectively; $\chi\geq 0$ is the rate measuring the strength of prey-taxis; K is the carrying capacity for the prey; β is the trophic efficiency. We consider the Holling type II functional response

$$f(u) = \frac{\alpha u}{1+\alpha h u}, \tag{A2}$$

and the case of Holling type I functional response is discussed in Remark A.1. In (A2), α is the capture rate and h is the handling time. All the parameters above are positive except $\chi\geq 0$. We shall show that in the presence of prey-taxis, Turing instability is impossible in the system (A1) with (A2). More general prey-taxis models involving (A1) have been considered in Jin and Wang (2017, 2021), where no spatial patterns are observed.

Clearly, the system (A1) with (A2) has the constant steady states

$$\begin{cases} E_0,\ E_1,\ E_*, & \text{if } \theta\in(0,\beta f(K)),\\ E_0,\ E_1, & \text{if } \theta\in[\beta f(K),\infty), \end{cases} \tag{A3}$$

where $E_0 = (0, 0)$ is the extinction steady state, $E_1 = (K, 0)$ the predator-free constant steady state, and E_* is the unique positive constant steady state with

$$E_* = \left(\frac{\theta}{\alpha(\beta - h\theta)}, \frac{\beta(\beta f(K) - \theta)}{\alpha f(K)(\beta - h\theta)^2} \right), \quad \text{if } \theta \in (0, \beta f(K)).$$

To investigate the linear stability of these constant steady states, we linearize the system (A1) at a constant steady state $E_s = (u_s, w_s)$ to get

$$\begin{cases} \Psi_t = \mathcal{M}\Delta\Psi + \mathcal{J}\Psi, & x \in \Omega, t > 0, \\ \partial_\nu \Psi = 0, & x \in \partial\Omega, t > 0, \\ \Psi(x, 0) = (u_0 - u_s, w_0 - w_s)^{\mathcal{T}}, & x \in \Omega, \end{cases}$$

where $\Psi(x, t) = (u - u_s, w - w_s)^{\mathcal{T}}$ and $\partial_\nu \Psi(x, t) = (\partial_\nu u, \partial_\nu w)^{\mathcal{T}}$ with $\mathcal{T}$ denoting the transpose, the two matrices $\mathcal{M} = \mathcal{M}(E_s)$ and $\mathcal{J} = \mathcal{J}(E_s)$ are given by

$$\mathcal{M} := \begin{pmatrix} d_1 & 0 \\ -\chi w_s & d_2 \end{pmatrix} \quad \text{and} \quad \mathcal{J} := \begin{pmatrix} 1 - \frac{2u_s}{K_1} - w_s f_1'(u_s) & -f_1(u_s) \\ \beta_1 w_s f_1'(u_s) & \beta_1 f_1(u_s) + \beta_2 f_2(v_s) - \theta \end{pmatrix}.$$

By similar arguments to those used in the derivation of (4.8), we obtain the characteristic equation

$$\rho_k^2 + A_1 \rho_k + A_0 = 0, \tag{A4}$$

where

$$\begin{cases} A_1 := \mu_k(d_1 + d_2) - tr(\mathcal{J}), \\ A_0 := d_1 d_2 \mu_k^2 + \Gamma \mu_k + Det(\mathcal{J}) \quad \text{with } \Gamma := -(d_1 J_{22} + d_2 J_{11} + \chi w_s J_{12}). \end{cases} \tag{A5}$$

Then the constant steady state E_s is linearly stable if and only if $A_1, A_0 > 0$ for all $k \geq 0$.

A.1 Stability analysis for the ODE (non-spatial) model

In the absence of spatial structure effects, the system (A1) becomes

$$\begin{cases} u_t = u\,(1 - u/K) - w f(u), & t > 0, \\ w_t = w\,(\beta f(u) - \theta), & t > 0, \end{cases} \tag{A6}$$

which has three possible equilibria given in (A3). The ODE system (A6) with the Holling type II functional response has been extensively studied, and we refer the readers to Hsu (2005); Yi et al. (2009) and the references therein. We have the following linear stability results for (A6) when $f(u)$ takes the specific form (A2).

Lemma A.1 *For the ODE system (A6) with (A2), we have the following stability results.*

(i) E_0 *is a saddle;*

(ii) E_1 *is linearly stable, marginally stable and linearly unstable for* $\theta > \beta f(K)$, $\theta = \beta f(K)$ *and* $\theta \in (0, \beta f(K))$, *respectively.*

(iii) If $0 < h \le \frac{1}{K\alpha}$, *then* E_* *is linearly stable for* $\theta \in (0, \beta f(K))$; *if* $h > \frac{1}{K\alpha}$, *then* E_* *is linearly stable, marginally stable and linearly unstable for* $\theta \in (\theta_0, \beta f(K))$, $\theta = \theta_0$ *and* $\theta \in (0, \theta_0)$, *respectively. Here,* $\theta_0 := \left[\frac{\beta(\alpha hK-1)}{h(\alpha hK+1)}\right]_+$.

Proof (i) Let $E_s = E_0$. Then the two eigenvalues of $\mathcal{J}$ are $-\theta$ and 1, which shows that E_0 is a saddle. (ii) Let $E_s = E_1$. Then the two eigenvalues of $\mathcal{J}$ are -1 and $\beta f(K) - \theta$, which proves the second result. (iii) Let $\theta \in (0, \beta f(K))$ and $E_s = E_*$. Then (A5) with $k = 0$ and $\mu_0 = 0$ shows that

$$A_1 = -tr(\mathcal{J}) = \frac{h\theta\left(\theta - \frac{\beta(\alpha hK-1)}{h(\alpha hK+1)}\right)}{\beta f(K)(\beta - h\theta)}, \quad A_0 = Det(\mathcal{J}) = \frac{\theta(\beta f(K) - \theta)}{\beta f(K)} > 0.$$

With the basic fact that $\theta < \beta f(K) = \frac{\beta\alpha K}{1+\alpha hK} < \frac{\beta}{h}$, we know that $sign(A_1) = sign\left(\theta - \frac{\beta(\alpha hK-1)}{h(\alpha hK+1)}\right)$. Then the third conclusion follows immediately. The proof is completed. □

A.2 Stability analysis for the spatial model

Turing instability means the constant steady state which is linearly stable in the non-spatial model becomes unstable in the presence of the spatial movement. In the case of $\alpha hK < 1$ (which is used for the hypothesis (H4) in Jin and Wang (2017)), (Jin and Wang 2017, Theorem 1.3) obtained the global stability of E_1 for $\theta > \beta f(K)$, and the global stability of E_* under certain parameter conditions (notably, Jin and Wang 2017 considered more general forms of functional responses and the prey growth functions including the case here). For the system (A1) with (A2) and general parameters, we next show that there is no Turing instability.

Lemma A.2 *There is no instability driven by diffusion or prey-taxis in the spatial system (A1) with (A2).*

Proof Given Lemma A.1, we only need to investigate the stability of E_1 for $\theta > \beta f(K)$, and the stability of E_* for $\theta \in (\theta_0, \beta f(K))$. We first let $E_s = E_1$, then the two roots of (A4) are $-1 - d_1\mu_k < 0$ and $-d_2\mu_k + \beta f(K) - \theta < 0$ for $\theta > \beta f(K)$, which shows that E_1 is linearly stable. It remains to consider the stability of E_* for $\theta \in (\theta_0, \beta f(K))$. Let $E_s = E_*$. Then Γ given by (A5) satisfies

$$\Gamma = \frac{\theta\left[\alpha h d_2(\beta - h\theta)\left(\theta - \frac{\beta(\alpha hK-1)}{h(\alpha hK+1)}\right) + \beta\chi(\beta f(K) - \theta)\right]}{\alpha\beta f(K)(\beta - h\theta)^2} > 0,$$

where we have used the fact that $\frac{\beta(\alpha hK-1)}{h(\alpha hK+1)} \le \theta_0 < \theta < \beta f(K) < \frac{\beta}{h}$ for $\theta \in (\theta_0, \beta f(K))$. Then (A5) along with Γ, $-tr(\mathcal{J})$, $Det(\mathcal{J}) > 0$ implies $A_1, A_0 > 0$.

Hence the two roots of (A4) have negative real parts and E_* is linearly stable. This completes the proof. □

Remark A.1 If the functional response $f(u)$ is of Holling type I

$$f(u) = \alpha u \tag{A7}$$

with a constant $\alpha > 0$, then there is no Turing instability in the system (A1) with (A7). The proof parallels the Holling type II case but requires simpler computations and it is omitted for brevity.

Acknowledgements The authors are grateful to the anonymous reviewers for their valuable comments, which greatly improved the exposition of the manuscript. The research of Y. Lou is partially supported by the NSF of China (No. 12261160366, No. 12250710674, No. 12426601). The research of W. Tao is partially supported by the NSF of China (No. 12201082), and PolyU Postdoc Matching Fund Scheme Project code P0030816/B-Q75G, 1-W15F and 1-YXBT. The research of Z.-A. Wang was partially supported by the NSFC/RGC Joint Research Scheme sponsored by the Research Grants Council of Hong Kong and the National Natural Science Foundation of China (Project No. N_PolyU509/22), and an internal grant 4-ZZRC from the Hong Kong Polytechnic University.

Funding Open access funding provided by The Hong Kong Polytechnic University

Data Availability The authors declare that the manuscript has no associated data.

Declarations

Conflict of interest The authors have no conflicts of interest to declare that are relevant to the content of this article.

References

Abrams PA (1999) Is predator-mediated coexistence possible inunstable systems? Ecology 80(2):608–621

Amann H (1993) Nonhomogeneous linear and quasilinear elliptic and parabolic boundary value problems. in function spaces, differential operators and nonlinear analysis. Teubner Stuttgart 133:9–126

Amann H (1990) Dynamic theory of quasilinear parabolic equations. II Reaction-diffusion systems Differ Integral Equ 3(1):13–75

Apreutesei N, Dimitriu G, Strugariu R (2014) An optimal control problem for a two-prey and one-predator model with diffusion. Comput Math Appl 67(12):2127–2143

Cai Y, Cao Q, Wang Z-A (2022) Asymptotic dynamics and spatial patterns of a ratio-dependent predator-prey system with prey-taxis. Appl Anal 101(1):81–99

Caswell H (1978) Predator-mediated coexistence: a nonequilibrium model. Amer Nat 112(983):127–154

Chailleux A, Mohl EK, Alves MT, Messelink GJ, Desneux N (2014) Natural enemy-mediated indirect interactions among prey species: potential for enhancing biocontrol services in agroecosystems. Pest Manag Sci 70(12):1769–1779

Chaneton EJ, Bonsall MB (2000) Enemy-mediated apparent competition: empirical patterns and the evidence. Oikos 88(2):380–394
Cosner C (2014) Reaction-diffusion-advection models for the effects and evolution of dispersal. Discrete Contin Dyn Syst 34(5):1701–1745
De Mottoni P (1979) Qualitative analysis for some quasilinear parabolic systems. Inst Math Polish Acad Sci Zam 190:11–79
De Mottoni P, Rothe F (1979) Convergence to homogeneous equilibrium state for generalized volterra-lotka systems with diffusion. SIAM J Appl Math 37(3):648–663
DeAngelis DL (2012) Dynamics of nutrient cycling and food webs, vol 9. Springer Science & Business Media, NY
DeCesare NJ, Hebblewhite M, Robinson HS, Musiani M (2010) Endangered, apparently: the role of apparent competition in endangered species conservation. Anim Conser 13(4):353–362
Dieckmann U, O'Hara B, Weisser W (1999) The evolutionary ecology of dispersal. Trends Ecology & Evolution 14(3):88–90
Du Y, Shi J (2006) Some recent results on diffusive predator-prey models in spatially heterogeneous environment. In Nonlinear dynamics and evolution equations, volume 48 of Fields Inst. Commun., pages 95–135. Amer. Math. Soc., Providence, RI
Dunn AM, Torchin ME, Hatcher MJ, Kotanen PM, Blumenthal DM, Byers JE, Coon CA, Frankel VM, Holt RD, Hufbauer RA, Kanarek AR, Schierenbeck KA, Wolfe LM, Perkins SE (2012) Indirect effects of parasites in invasions. Funct Ecol 26(6):1262–1274
Feng W (1993) Coexistence, stability, and limiting behavior in a one-predator-two-prey model. J Math Anal Appl 179(2):592–609
Haskell EC, Bell J (2020) Pattern formation in a predator-mediated coexistence model with prey-taxis. Discrete Contin Dyn Syst Ser B 25(8):2895–2921
He X, Ni W-M (2016) Global dynamics of the lotka-volterra competition-diffusion system: diffusion and spatial heterogeneity I. Comm Pure Appl Math 69(5):981–1014
George E (2017) Heimpel and Nicholas J. Cambridge University Press, Mills, Biological control
Hiltunen T, Laakso J (2013) The relative importance of competition and predation in environment characterized by resource pulses-an experimental test with a microbial community. BMC Ecol 13(1):1–8
Holt RD (1977) Predation, apparent competition, and the structure of prey communities. Theor Popul Biol 12(2):197–229
Holt RD, Bonsall MB (2017) Apparent competition. Annu Rev Ecol Evol Syst 48(1):447–471
Holt RD, Polis GA (1997) A theoretical framework for intraguild predation. Amer Nat 149(4):745–764
Hsu S-B (1981) Predator-mediated coexistence and extinction. Math Biosci 54(3):231–248
Hu B (2005) A survey of constructing lyapunov functions for mathematical models in population biology. Taiwanese J Math 9(2):151–173
Hu B (2011) Blow-up theories for semilinear parabolic equations, vol 2018. Lecture Notes in Mathematics, Springer, Heidelberg
Huang Y-L, Lin G (2014) Traveling wave solutions in a diffusive system with two preys and one predator. J Math Anal Appl 418(1):163–184
Jin H-Y, Wang Z-A (2017) Global stability of prey-taxis systems. J Differ Equ 262(3):1257–1290
Jin H-Y, Wang Z-A (2021) Global dynamics and spatio-temporal patterns of predator-prey systems with density-dependent motion. European J Appl Math 32(4):652–682
Karban R, Hougen-Eitzmann D, English-Loeb G (1994) Predator-mediated apparent competition between two herbivores that feed on grapevines. Oecologia 97(4):508–511
Kaser JM, Ode PJ (2016) Hidden risks and benefits of natural enemy-mediated indirect effects. Curr Opin Insect Sci 14:105–111
Lakoš N (1990) Existence of steady-state solutions for a one-predator-two-prey system. SIAM J Math Anal 21(3):647–659
Gary M (1996) Lieberman. Second order parabolic differential equations. World Scientific Publishing Co., Inc, River Edge, NJ
Lou Y (2006) On the effects of migration and spatial heterogeneity on single and multiple species. Differential Equations 223(2):400–426
Lou Y, Tao W, Wang Z-A (2025). Effects and biological consequences of the predator-mediated apparent competition I: ODE models. J Math Biol 91:47, 37 pages
Manna K, Volpert V, Banerjee M (2020) Dynamics of a diffusive two-prey-one-predator model with nonlocal intra-specific competition for both the prey species. Mathematics 8(1):101

Mimura M, Kan-on Y (1986) Predation-mediated coexistence and segregation structures. Stud Appl Math 18:129–155
Murray JD (2002) Mathematical Biology I: An introduction, volume 17 of Interdisciplinary Applied Mathematics. Springer-Verlag, New York, third edition
Piltz SH, Veerman F, Maini PK, Porter MA (2017) A predator-2 prey fast-slow dynamical system for rapid predator evolution. SIAM J Appl Dyn Syst 16(1):54–90
Polis GA, Winemiller KO (2013) Food webs: integration of patterns & dynamics. Springer Science & Business Media, NY
Ron R, Fragman-Sapir O, Kadmon R (2018) Dispersal increases ecological selection by increasing effective community size. Proc Nat Acad Sci 115(44):11280–11285
Shurin JB, Allen EG (2001) Effects of competition, predation, and dispersal on species richness at local and regional scales. Amer Nat 158(6):624–637
Song Y, Tang X (2017) Stability, steady-state bifurcations, and turing patterns in a predator-prey model with herd behavior and prey-taxis. Stud Appl Math 139(3):371–404
Stige LC, Kvile KØ, Bogstad B, Langangen Ø (2018) Predator-prey interactions cause apparent competition between marine zooplankton groups. Ecology 99(3):632–641
Strauss A, White A, Boots M (2012) Invading with biological weapons: the importance of disease-mediated invasions. Funct. Ecol. 1249–1261
Tilman D (1987) The importance of the mechanisms of interspecific competition. Amer Nat 129(5):769–774
Vance RR (1978) Predation and resource partitioning in one predator-two prey model communities. Amer Nat 112(987):797–813
Wang M (2018) Note on the lyapunov functional method. Appl Math Lett 75:102–107
Wittmer HU, Robert SL, Elbroch M, Marshall AJ (2013) Conservation strategies for species affected by apparent competition. Conserv Biol 27(2):254–260
Wu CC (2019) The spreading speed for a predator-prey model with one predator and two preys. Appl Math Lett 91:9–14
Yi F, Wei J, Shi J (2009) Bifurcation and spatiotemporal patterns in a homogeneous diffusive predator-prey system. J Differential Equations 246(5):1944–1977